UNIVERSITÄT AUGSBURG
Universitätsbibliothek

OPEN ACCESS
OPUS AUGSBURG

Turbomachinery component manufacture by application of electrochemical, electro-physical and photonic processes

Fritz Klocke, Andreas Klink, Drazen Veselovac, David Keith Aspinwall, Sein Leung Soo, Michael Schmidt, Johannes Schilp, Gideon Levy, Jean-Pierre Kruth

Angaben zur Veröffentlichung / Publication details:

Klocke, Fritz, Andreas Klink, Drazen Veselovac, David Keith Aspinwall, Sein Leung Soo, Michael Schmidt, Johannes Schilp, Gideon Levy, and Jean-Pierre Kruth. 2014. "Turbomachinery component manufacture by application of electrochemical, electro-physical and photonic processes." *CIRP Annals* 63 (2): 703–26. https://doi.org/10.1016/j.cirp.2014.05.004.

Nutzungsbedingungen / Terms of use:

CC BY-NC-ND 4.0

Dieses Dokument wird unter folgenden Bedingungen zur Verfügung gestellt: / This document is made available under these conditions:
CC-BY-NC-ND 4.0: Creative Commons: Namensnennung - Nicht kommerziell - Keine Bearbeitung
Weitere Informationen finden Sie unter: / For more information see:
https://creativecommons.org/licenses/by-nc-nd/4.0/deed.de

Turbomachinery component manufacture by application of electrochemical, electro-physical and photonic processes

Fritz Klocke (1)[a], Andreas Klink[a,*], Drazen Veselovac[a], David Keith Aspinwall (1)[b], Sein Leung Soo (2)[b], Michael Schmidt (3)[c], Johannes Schilp[d], Gideon Levy (1)[e], Jean-Pierre Kruth (1)[f]

[a] *Laboratory for Machine Tools and Production Engineering, WZL, RWTH Aachen University, Aachen, Germany*
[b] *Machining Research Group, School of Mechanical Engineering, University of Birmingham, Birmingham, United Kingdom*
[c] *Bayerisches Laserzentrum GmbH, BLZ, Erlangen, Germany*
[d] *Institute for Machine Tools and Industrial Management IWB, Technische Universität München, München, Germany*
[e] *Centro Para o Desenvolvimento Rapido e Sustentado de Produto CDRSP, Instituto Politecnica de Leiria IPL, Leiria, Portugal*
[f] *Division PMA (Production Engineering), University of Leuven (KU Leuven), Leuven, Belgium*

1. Introduction

The demand for turbomachinery systems such as aero-engines, stationary gas and steam turbines as well as turbochargers for engines is constantly growing due to the increasing worldwide requirement for energy and mobility. In contrast, conventional energy resources such as oil, gas and coal together with important raw materials are shrinking while environmental pollution due to CO_2 and NO_x emissions is on the rise. Thus, energy and fuel prices as well as costs for environmental protection and sustainability are constantly increasing, necessitating the development and introduction of highly efficient turbomachinery systems.

Taking the aerospace sector as an example, air traffic is resiliently growing at a rate of 4–5% a year both for revenue passenger (RPK) as well as cargo traffic tonne kilometres (RTK), practically doubling within 15 years. According to the 'Global Market Forecast 2012-32', Airbus predicts a doubling of the passenger aircraft fleet ($\geq$ 100 seats: single/twin-aisle and very large) from 16,094 to 33,651 by 2032. Including replacements, some 28,355 new aircraft deliveries are anticipated. Similar numbers are presented in Boeing's 'Current Market Outlook 2013-32' showing the 20,310 aircraft (regional jets, single aisle, small/medium/large widebody) currently in service increasing to 41,240 by 2032 with new deliveries of 35,280 [29,86,123]. In terms of aeroengines, Rolls-Royce expects ~68,000 deliveries (including business jets) over the period 2012-31, with a market value of $975 billion [164]. Adding to this, the servicing of commercial engines involving maintenance, repair and overhaul (MRO) is also growing in importance. Within GE Aviation, the service market for 2011 amounted to $7.2 billion while the new engine market was $4.9 billion [100].

Besides market growth, the challenges faced by industry are also growing, because future aircraft including the engines must also be more fuel efficient, quieter and cleaner due to official regulations and agreements. The new ACARE (Advisory Council for Aviation Research and Innovation in the EU) goals for 2050, schedule a reduction of 75% in CO_2, 90% in NO_x and 65% in noise relative to 2000 [2,86]. In summary, there is an extensive and pressing need for design – as well as advanced manufacturing and repair technologies able to handle the current and growing future demands for turbomachinery components.

2. Challenges of turbomachinery component manufacture

Core functional components of turbomachinery systems are characterised by the use of dedicated high temperature, high specific strength and wear-resistant materials (Fig. 1).

* Corresponding author.
E-mail address: a.klink@wzl.rwth-aachen.de (A. Klink).

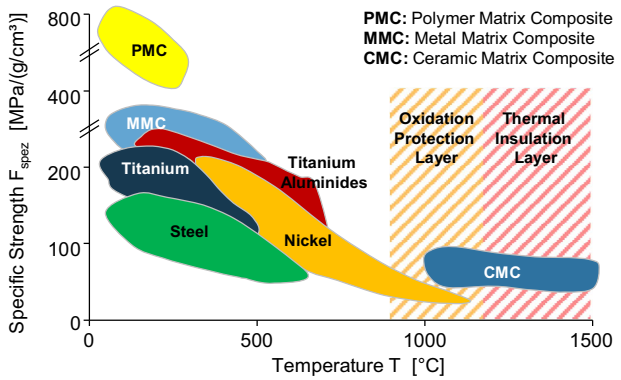


Fig. 1. Specific strength of materials as a function of working temperature for turbomachinery components. Based on [181].

Machining such "difficult-to-cut" materials using conventional means is very challenging, often resulting in low material removal rates (MRR), reduced precision due to high cutting forces, high tooling costs due to increased wear and consequently low process efficiency [178]. In addition, the resulting surface integrity is often characterised by thermo-mechanically altered or even damaged rim zones [97,178,196]. Thus, the utilisation of technological as well as economically suitable manufacturing technologies is of great interest.

Taking the aerospace sector again as an example, Fig. 2 shows the specific areas of application for preferred Ti and Ni-based alloys in aeroengines. The temperature capability of such materials is constantly increasing through the development of new materials with different primary manufacturing technologies [158] (Fig. 3). Due to the absence of grain boundaries, single crystal materials exhibit far better creep properties than polycrystalline materials and can therefore be utilised at higher temperatures [34]. The use of such new materials and especially the advanced gamma titanium aluminides (for compressor as well as turbine applications) [13] and polymer matrix composites – PMC (for fan blading components), (Fig. 2), require amongst others, the development of appropriate manufacturing technologies.

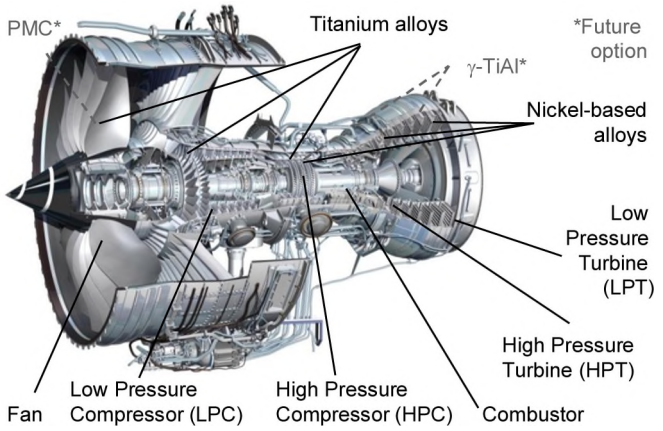


Fig. 2. Current and future temperature specific application of materials in aero engines (example: Rolls Royce Trend 800 engine).

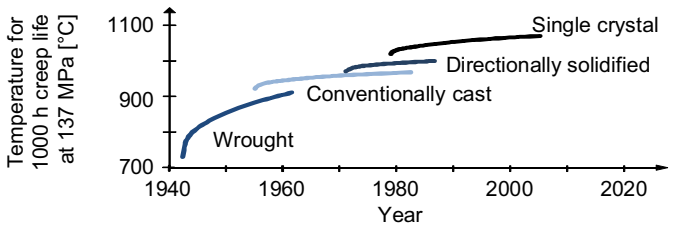


Fig. 3. Evolution of high-temperature strength capability of turbine blading nickel-based super alloys. Based on [158].

The most important turbomachinery steel, Ti- and Ni-based materials discussed in this paper are:

- *Steel alloys*: X22CrMoV211; X12CrNiWTiB16-13
- *Ti-based alloys*: Ti–6Al–4V (Ti64/Ti6Al4V); Ti–6Al–2Sn–4Zr–2Mo–0.1Si (Ti6242); Ti6246; Ti–5Al–2Sn–2Zr–4Mo–4Cr (Ti17)
- Gamma titanium aluminides (γ-TiAl): TNM; GE 48-2-2; 45 XD
- *Ni-based superalloys*: Inconel 718** (In718); In718 DA***; IN100**; Inconel 738**; Inconel 939**; MAR-M002°; MAR-M247°; Waspalloy*; Udimet 720*; Nimonic 105*; Nimonic 713*; Rene88**; RR1000°*; CMSX4°°; LEK94°°

Legend: *wrought, **cast, °directionally solidified,°°single crystal,°* powder metallurgical, ***direct aged

In order to increase aeroengine economic and ecological efficiency, current focus centres on the enhancement of propulsive as well as thermal effectiveness [31,98,198]. Propulsive efficiency can mainly be improved by realisation of higher by-pass ratios such as via the concept of Geared Turbo Fans [81]. Due to limited ground clearance of aircraft (classical design) and therefore limited fan diameters, the core engine has subsequently also to be reduced in size. The thermal efficiency can be further increased through higher temperature combustion requiring new high temperature resistant and lightweight materials (e.g. graded materials, single crystal, metal matrix composites – MMC and ceramic metal composites – CMC) and better cooling concepts (new cooling hole geometries, double walled bladings) as well as thermal barrier coatings (TBC) [32,64,175,180,181]. As a consequence, the need for more Ni-based compressor/turbine stages can be expected. Additionally, improved aero-dynamic and lightweight construction designs involving "hyper-polished" airfoils, elliptical leading/trailing edges or blisk manufacture, (Fig. 4), can further increase stage pressure ratios and thus efficiency [36,38].

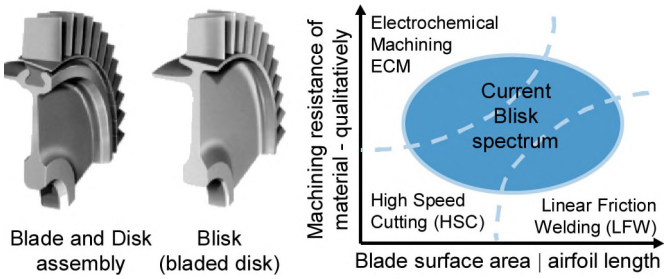


Fig. 4. Blisk principle design [163] and exemplarily, qualitative classification of currently used machining technologies as a function of blade surface are size (and airfoil length) and material machinability, [36].

In order to overcome current manufacturing limitations of conventional machining and to extend the potential of Design For Manufacture (DFM), an evaluation of the capabilities of advanced, non-mechanical, single process technologies, as well as new process chains both for initial manufacture and repair is necessary [37]. Comparing e.g. milling and ECM (Fig. 5), the MRR is reduced hyperbolical with the cutting tool overhang while constantly increasing with the ECM working area for comparable axis scales during blisk slot roughing. Besides productivity, the criticality of aeroengine failures necessitates appropriate workpiece surface integrities [196]. Also, economic capabilities have to be evaluated against the background of constantly growing volumes in turbomachinery serial production [22].

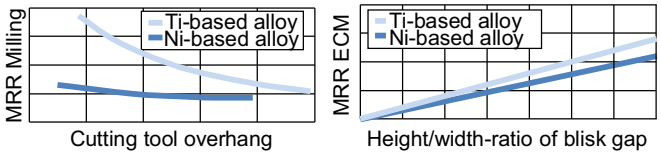


Fig. 5. Conceptual qualitative comparison of technological potential of conventional milling and ECM for machining of blisk blading gaps.

The paper reviews comprehensively the past, current and future technological and economical capabilities of ECM, EDM and photonic (laser/EBM) additive and subtractive processes for turbomachinery component manufacture. It focusses on the description of shaping processes excluding pure welding or coating applications. As the machining of composite materials (PMC, MMC, CMC) with electrically non-conductive phases cannot be executed using ECM/EDM and is generally inefficient with lasers, the paper focusses on the machinability analysis of steel, Ti and Ni-based alloys.

3. Technological capabilities of advanced processes

3.1. Electrochemical machining (ECM)

3.1.1. Introduction

The major advantages of ECM are its process specific characteristics of high material removal rate in combination with almost no tool wear. Due to cost intensive tool pre-developing processes and rather high investment outlays for the machine tools however, ECM is specifically used in large batch size production and represents an alternative manufacturing technology for turbomachinery components. In addition, high material removal rates can be realised while achieving good workpiece surface quality without the occurrence of white layers, heat affected zones or strain hardening [104,110,112]. This section gives a specific overview on the technological capabilities for the production of different geometrical features of turbomachinery components.

3.1.2. Material specific removal rates and resulting surface integrity

Independent of the type of ECM process – direct current (DC) or electrically and mechanically pulsed processes (PECM) – material removal is only dependent on the electrochemistry of the workpiece materials in combination with the electrolyte and the programmed current densities. For ECM tool design, it is necessary to know the local gap details during the process. The local gap width can initially be calculated with a combination of Ohm's and Faraday's law (for complex shaped geometries and long flow lengths the approximation loses its validity). Eq. (1) shows the effective material removal rate V_{eff} based on the specific removal rate $V_{sp,alloy}$ according to Faraday's law reduced by the current efficiency η [104]. In the pure form of Faraday's law, only one electrochemical valency is considered for each element and the equation has to be corrected by η, which also can be considered as an efficiency factor. Furthermore, the calculation of local effective gap s_{eff} by the combination of Ohm's and Faraday's law is only applicable in the frontal gap [104]. For complex shaped geometries, it can roughly be corrected by the angle of inclination of the workpiece contour α (Eq. (2)), [112].

$$V_{eff} = V_{sp,alloy} \cdot \eta = \frac{\eta}{\rho_{alloy}} \cdot \sum_{i=1}^{n} \frac{w_i}{100} \cdot \frac{M_i}{z_i \cdot F} \tag{1}$$

$$s_{eff,\alpha} = \frac{(U - \Delta U) \cdot V_{eff} \cdot \kappa}{\upsilon_f \cdot \sin\alpha} = \frac{(U - \Delta U) \cdot V_{eff} \cdot \kappa}{\upsilon_f \cdot \sqrt{1 - \cos^2\alpha}} \tag{2}$$

In practice, it is necessary to experimentally determine the effective material removal rate by analysing the behaviour of feed rate as a function of current density. Typical results are shown in Fig. 6 for the DC-machining of cylindrical holes with a tool diameter of 6 mm and internal flushing.

The linear behaviour and zero dependence of electrolyte concentration on effective material removal rate are typical of ECM processes at high current densities. Fig. 7 summarises the averaged effective material removal rates of relevant turbomachinery alloys. The linear curves were combined into a single function denoted as $V_{eff,Ø}$, which is the averaged effective material removal rate. All of the titanium alloys had a near identical $V_{eff,Ø}$ of ~1.78 mm³/(A min). In the case of nickel-based alloys, finer grained microstructures lead to better electrochemical machinability and faster dissolution. Consequently, superalloys manufactured via powder metallurgy (PM) techniques show the best electrochemical machinability. In general, nickel-based alloys dissolve faster than titanium alloys [112].

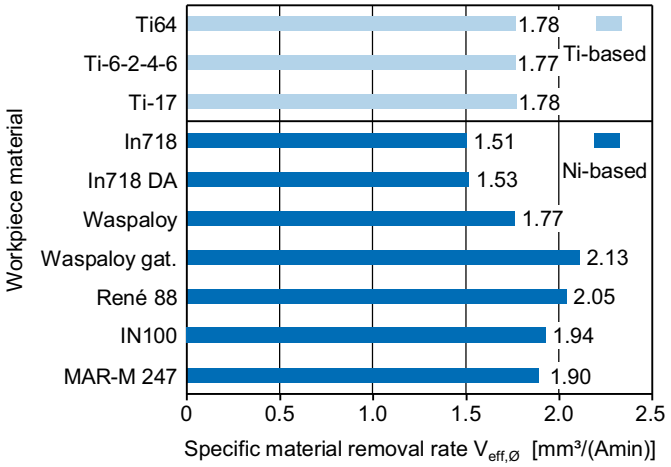
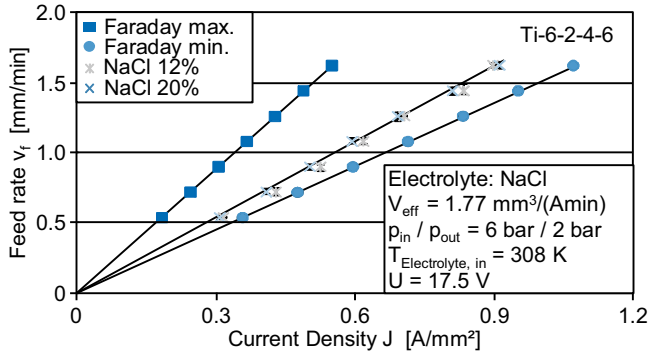


Fig. 7. Averaged effective material removal rates for different titanium- and nickel-based alloys, [112].

Besides the proportional interrelationship between feed rate v_f (equal to the resulting dissolution velocity v_A) and current density, hyperbolic interrelationships can be identified for the frontal gap size s_{90} ($s_{eff,\alpha}$; $\alpha = 90°$) as well as the resulting surface roughness (Ra) and the current density [110]. Therefore, high material removal rates can in principle be achieved simultaneously with small frontal gap sizes which give the highest precision while also producing low surface roughness for surface smoothing and polishing effects. Fig. 8 shows results for the machining of Ti–6Al–4V and Inconel 718.



Element	Al	Zr	Sn	Mo	Ti
weight % max.	6.5	4.5	2.25	6.5	80.25
weight % min.	5.5	3.5	1.75	5.5	83.75
valency z max.	3	4	4	6	3
valenzy z min.	3	4	2	6	1

Fig. 6. Experimental result of feed rate depending on current density of Ti-6-2-4-6 in comparison to Farady's law, [112].

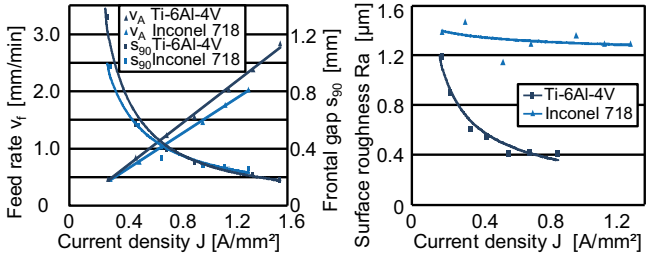


Fig. 8. Machining characteristics – feed rate, frontal gap size and resulting surface roughness depending on current density, [110].

The fact that the hyperbolic response of Inconel 718 is not as pronounced as Ti–6Al–4V is a result of the specific microstructure of the nickel-based alloy employed. Such curve relationships mean that higher feed rates can be used to produce advanced surface quality at the front edge. Conversely, the surface quality at the lateral area of 3D-structures declines with low current densities [110].

The resulting microstructure of the part surfaces after ECM strongly depends on the specific composition of the bulk material. Although no thermally damaged or mechanically deformed rim zones occur with ECM, different material phases or crystallographic orientations of the alloys have different electrochemical dissolution behaviours (up to inter-crystalline and pitting corrosion) resulting in different removal speeds [179]. Depending on the size of the phases and different heat treatment – a defined roughness or waviness of the surface can result following ECM.

Fig. 9 gives an overview on surface integrities of different materials after specific electrochemical treatments. For Inconel 718 and Inconel 718 DA which has a more fine-grained microstructure, a smooth and flat surface finish without any rim zone can be seen in the cross sections when employing optimised ECM parameters. For Ti–6Al–4V, a slightly faster dissolution of the α-phase is visible in the detailed cross section with higher magnification showing a slight waviness – but without any rim zone – of the surface. For γ-TiAl machining, overlaying α_2-lamellas with thicknesses of <2 μm (due to a much reduced dissolution velocity [21]) results in high roughness after ECM shown in the detailed top view of the surface.

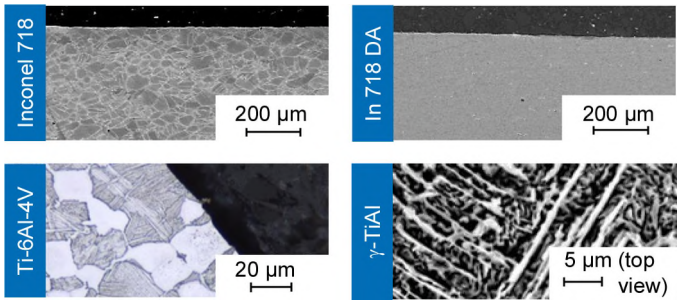


Fig. 9. Achievable surface integrity for different titanium and nickel-based alloys after ECM machining. Based on [21,112].

3.1.3. *New process modelling approaches*

The main reasons for high tooling costs with ECM are the reliance on only knowledge-based, iterative cathode designing process. After a test run the workpiece has to be measured and the difference between target and actual geometry is subtracted from the cathode and so forth, yet the theoretical background of the ECM process with all its different physical aspects, cf. Fig. 10, is well known [30,109].

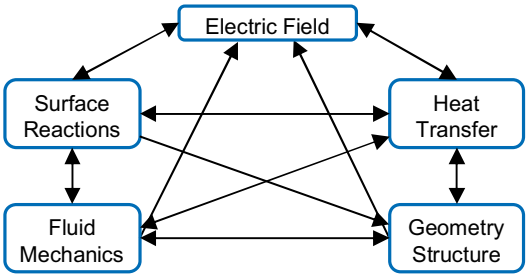


Fig. 10. Various physics coupling in modelling of ECM processes. Based on [110,194].

Improvements in computing power and simulation tools allow "multi-physics" approaches to simulate the complex ECM processes in one comprehensive approach. Thus, it will be possible in the future to combine different physical phenomena such as fluid flow, electric fields, heat transfer and surface reactions in one simulation [108]. Different new simulation approaches (e.g. for blading manufacture) are now being implemented for the first time and will be further improved.

The 2D-simulation of the DC-ECM manufacture of blades is shown in Fig. 11. The cathodes with a pre-machined geometry are moved with a constant feed rate towards the blade and due to the local conditions of electrolysis, the blade is formed. The simulation results show that the flow surfaces are closely mapped (maximum deviation <10 μm) in comparison to the experimental target geometry. Geometrical deviations of the order of 200 μm for trailing and leading edge can be explained by inaccuracies of the pre-determined inflow conductivity and inaccuracies in spline generation [109]. These deviations can be further minimised by optimisation steps. The final goal will be the implementation of an inverse simulation to predict the correct cathode shape depending on a given anode (blade) geometry [87].

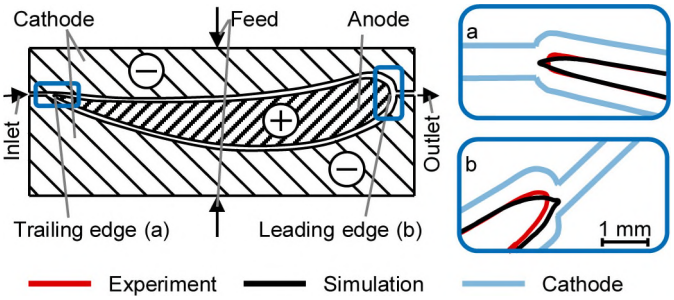


Fig. 11. Principle of ECM blade manufacture and according results of a 2D multi-physics simulation. Based on [109].

In Fig. 12 a comparison between experimental results, two different 3D multi-physics simulations and the established cos(φ)-method (sin(φ) alternatively, cf. Eq. (2) and [87]) is shown for the DC-ECM sinking of a leading edge rounded cuboid.

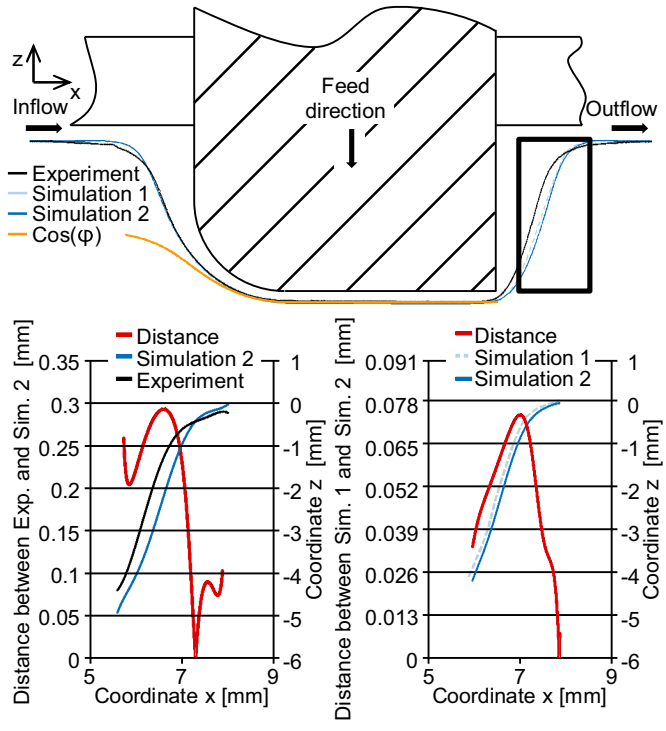


Fig. 12. Modelling performance dependence on integration level of physical effects and comparison to experiment, [108].

Here the cos(φ)-method can predict the anode shape only for small contour angles, below 40° and therefore shows the limited capabilities of conventional ECM simulation approaches. The contour of Simulation 1 in contrast is achieved by computing the electric field in conjunction with the Faraday model. In Simulation 2 heat transfer and fluid flow are also modelled [108]. It can be seen that both simulated results show good agreement with the experiment at the inflow and the frontal gap area. Downstream, after the cathode's sharp edge, the deviations between the contours grow (shown in black box). The largest difference between the calculated and the experimental result is located in the side gap at the outflow position. The maximum deviation between the experimental and simulated results is below 300 μm. In general, the material dissolving in the simulation is slightly higher than in the experiment. This effect is caused by neglecting the hydrogen evolution, which would gradually reduce the conductivity of the electrolyte in the direction of flow. Comparing the results from both simulations, it can be stated that because of Joule heating and the linear correlation of conductivity and temperature, material removal rate is higher for Simulation 2, [108]. The approaches presented clearly show the large potential of multi-physics simulation for implementing and optimising computer-aided cathode design.

3.1.4. Pulsed electrochemical machining (PECM)

For the achievement of higher precision and better surface qualities during ECM, pulsed process modifications have been developed since about 2000. Pulsed (also termed "precise") ECM (PECM) is a vibration assisted development of ECM die-sinking by applying a low frequency oscillation of the tool electrode within the working gap [122,168]. Using the combination of an additionally pulsed, high current density direct current and an oscillating electrode enables precise machining at reduced working gaps of about 10 μm to 100 μm compared to typical values of 100–1000 μm during DC-ECM with surface roughnesses down to Ra = 20–30 nm [35]. Depending on the workpiece material, even polished surfaces can be achieved via ECM. The principle of PECM is shown in Fig. 13.

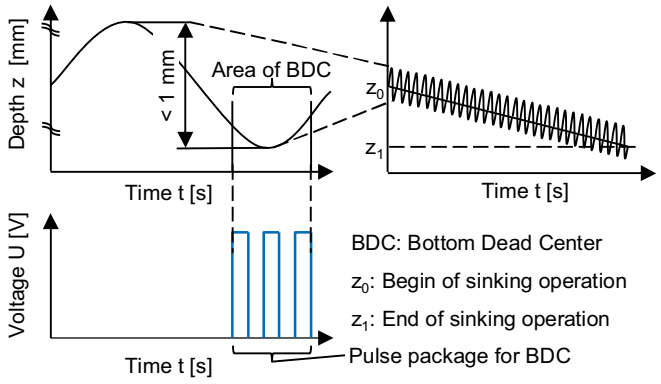


Fig. 13. Principle of Pulsed (Precise) Electrochemical Machining (PECM) with oscillating cathode tool electrode.

Due to the off-times in PECM, a considerable amount of the process time is used for the replacement of the electrolyte in the pulse pauses. In these pauses, no removal process takes place. Hence, the maximum removal rates of PECM compared to EC methods, in which continuous DC current is used, are significantly reduced (e.g. 20 times longer machining times [152]). However, due to refreshment of the fluid the electrochemical conditions within the working gap are kept much more constant. Therefore, for long fluid flow paths such as during the machining of blades or other macro geometrical features of turbomachinery components, gap widening effects over the flow channels length are significantly reduced. Thus, a more uniform gap size distribution is achieved allowing more precise machining and also simplification of tool electrode development iterations. In addition, during off-times the electrolyte saturation level with ions is reduced, allowing the application of higher current densities during on-times compared to DC applications. Another advantage is the fact that due to the high current densities in the small frontal gaps, reduced stray currents occur and lower etching attack next to the machining areas takes place [152].

3.1.5. Specific machine tools and process handling technology

Modern PECM machine tools allow roughing, finishing and polishing on one platform [63]. Fig. 14 shows such a machine tool with typically 7–8 axis (3–4 axis for the manipulation of the workpiece and 4 axis for tool movement (2 oscillating cathodes) [152]). The machine tool consists of a compact and closed system with autonomous electrolyte management.

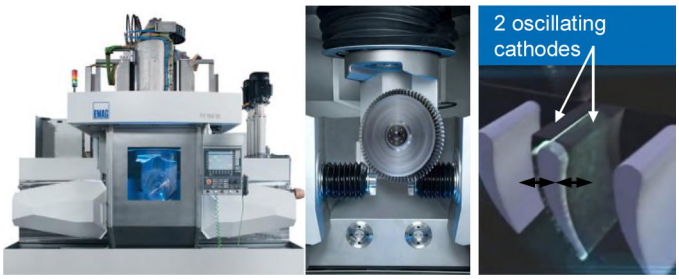


Fig. 14. PECM machine tool for rough and finish machining of blisk geometries with 2 vibrating cathode tool electrodes [59,74].

For the machining of titanium-based alloys, the electrolyte is typically aqueous solution of NaCl (avoiding passivation phenomena) while for nickel-based superalloys and TiAl, $NaNO_3$ is used. Fluid flow rates up to 1000 l/min and pressures up to 40 bar are realised in a closed-loop system with control of temperature and pH-value (via acid-/base-dosage) [59]. In addition, a monitoring and chemical treatment of chromium VI (reduction to chromium III) is nowadays implemented [195]. For filtering of the hydroxide precipitation usually back-flushable slurry filter membranes and chamber filter presses are used [59]. Finally, recycling and/or disposal have to be managed by certified specialists. Resulting costs for the electrolyte handling and the recycling/disposal of the slurry have therefore to be taken into account when considering machine investment and operation. An ecologically acceptable and user-friendly ECM process can then be realised.

The electrical power supply usually features scalable generator technology with up to 40 kA at pulse frequencies up to 10 kHz [59]. During roughing operations with constant DC, current densities of up to 3 A/mm^2 can successfully be applied allowing sufficient eduction of ions within the electrolyte [179]. Scaling with large area ECM (up to 60 cm^2 [20]) achieves high material removal rates but fluid flow paths have to be kept as short as possible in order to guarantee a fast electrolyte exchange. Additionally, tool systems including fluid chambers with inlet and outlet pressures have to be designed in such a way that flow striations due to unsteady flow can be avoided. Typically, feed rates of up to 3 mm/min are possible [35]. Fig. 15 shows machine set-ups for blade and blisk

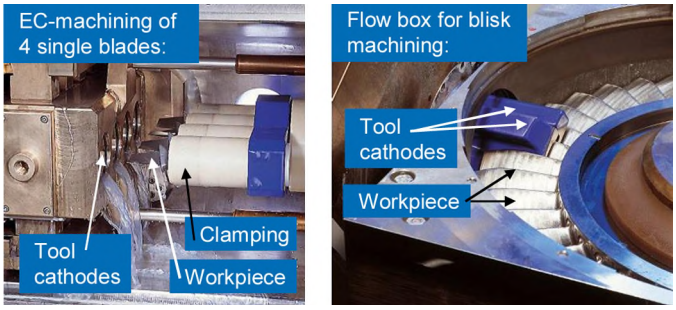


Fig. 15. Machine set-up for blade (left) and blisk (right) manufacture (DC-ECM), Leistritz Turbomaschinen Technik LTT [104].

manufacture (DC-ECM). On the left, the simultaneous machining of 4 blades is presented. The feed rate is independent of the area to be machined enabling a significant increase in productivity [61]. On the right the blisk fluid flow box which is completely flooded during machining is shown together with the tool electrodes.

The mechanical tool oscillators of PECM have typical amplitudes of 100 mm at frequencies of up to 100 Hz. During mechanically pulsed machining, typical feed rates are only 0.1 mm/min. Therefore, the PECM process is mainly used for finish machining and it becomes economic if it is combined with preliminary steps of DC-ECM [35,152]. In addition to providing high material removal rates and low surface roughness, both ECM and PECM produce burr-free geometries independent of shape complexity [73].

Once a process is configured and all electrical and fluid process parameters are maintained, excellent repeatability can be achieved. During machining of a blisk with 75 blades, 43 c_p values (defined as the number of times the spread of the process fits into the tolerance band) describing different geometrical features for blade position and thickness, chord length and line angles, thickness as well as geometry of leading and trailing edges, were analysed. All values were better than 1.3 and only one was lower than 1.33 (4σ). Maximum c_p index values were around 6.65 indicating a highly stable process [152].

3.1.6. *Examples for successful technological applications*

This section gives an overview of different successful application examples of ECM and PECM for the manufacture of turbomachinery components including information on relevant process conditions and achievable machining performance.

ECM is capable of producing single blade and vane geometries of different shapes both for aircraft engine and stationary steam and gas turbine applications (Fig. 16). During DC-ECM machining typical material removal can be several cm^3/min for different steel-based (e.g. X12CrNiWTiB16-13: 2.5 cm^3/min), titanium-based (e.g. Ti6242: 3.9 cm^3/min) and nickel-based (e.g. Inconel 718: 2.1 cm^3/min) alloys [20,72]. Form accuracy and surface roughness values of 0.1 mm and Ra = 0.8 μm respectively are possible. Calculated savings during manufacture of single blades amounts to 30% in comparison to cutting operations [35]. This is especially so in continuous production due to reduced tooling costs. Besides machining of free-form aerofoil shapes the process is also capable of machining the annulus with varying fillet radii and elliptical edges [20]. Further increase of productivity is possible during subsequent process optimisation [55]. The introduction of forged or cast TiAl blades in future engines will add even more significance to ECM [93].



Fig. 16. EC machining of blades and vanes for aerospace and stationary gas and steam turbine applications, [20,43,72].

Fig. 17 shows the machine set-up for the DC-ECM machining of blading on steel rotor shafts for stationary gas and steam turbines. The workpiece (X22CrMoV211) has a total length of 2300 mm and a diameter of 600 mm In total 120 blades are machined from 2 solid pre-turned shoulders of the shaft. Each blade is manufactured

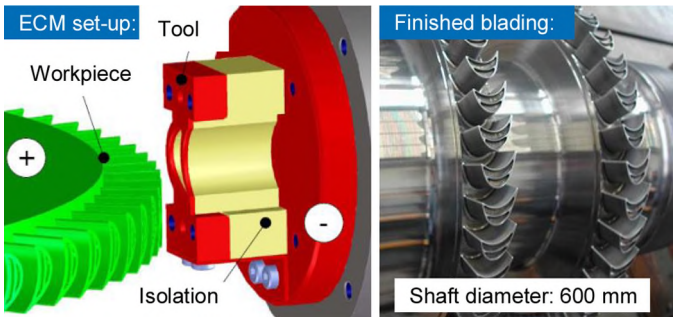


Fig. 17. EC machining of blades on steel (X22CrMoV211) rotor shafts for stationary gas and steam turbine applications [60,62].

by a radial movement of a sheet electrode which is isolated underneath the tool in order to avoid extensive side gap widening. The feed rate amounts to 3 mm/min [62].

The EC-machining of structural components like blade flanges on jet-engine casings (diameter of 350 mm, height of 350 mm) as well as machining to facilitate weight reduction at bolt holes on disks is presented in Fig. 18. In both cases, nickel-based alloys are machined via constant DC-ECM with working voltages of 20 V and 14 V and operating currents of 15 and 12 kA respectively [62].

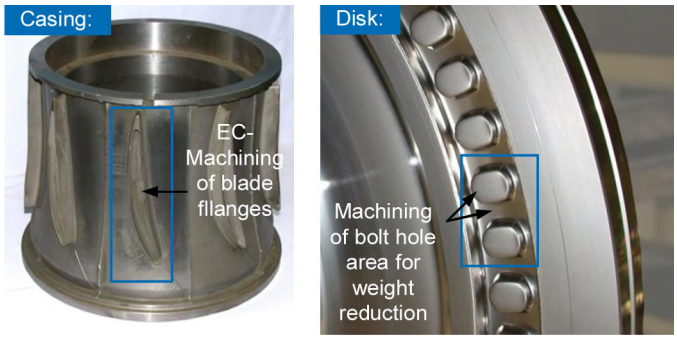


Fig. 18. EC-machining of blade flanges on jet-engine casing (left) and weight reduction at bolt holes on turbine disc (right), [62].

Fig. 19 shows an EC-machined titanium-based low pressure compressor blisk (Ti–6Al–4V) and the associated copper tool electrodes. The part has a diameter of 650 mm and incorporates 40 blades with a length of 100 mm and a profile length of 72 mm in total. It was pre-milled with an oversize of 2 mm. For the DC process NaCl was used as the electrolyte with current densities of 0.5–1 A/mm^2.

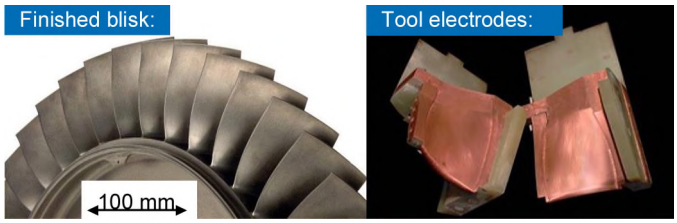


Fig. 19. Low pressure compressor blisk out of Ti6Al4V machined via ECM, [62,179].

Operating voltages of 13–18 V, currents of 12–15 kA and a feed rate of 1 mm/min resulted in total machining time of 5 min per blade [62,104,181].

Continuous developments in cutting technology has outpaced the application of ECM for the machining of Ti-based blisks but it is still very competitive for machining of Ni-based alloys (cf. Section 4). In order to obtain the best surface qualities of aerofoils, a combination of ECM roughing and PECM finishing is suggested, the approach developed from machining a nickel-based high pressure (HP) compressor blisk made from Inconel 718 (application: preparation for series production of PW6000 HPC stage 8). The design includes thin, heavy warped blades which would be very

difficult to be conventionally milled but represent ideal contours for ECM machining technologies using $NaNO_3$ as electrolyte. The machining sequence comprises DC ECM pre-machining of basic slots between the blades starting from a turned raw part. The machine set-up and the tool electrode are shown in the upper part of Fig. 20. The oversize around each blade is unequal and differs from about 1–3 mm. Sufficient gap is necessary between two blades in order to accommodate the finishing electrodes. This process is followed by an unpulsed ECM roughing step to an equidistant oversize. After this, the leading and trailing edges are prepared. In the last step, PECM finishing with oscillating tool electrodes takes place to finalise the aerofoils and annulus. The machining set-up and electrodes are shown in the lower part of Fig. 20 [55,152].

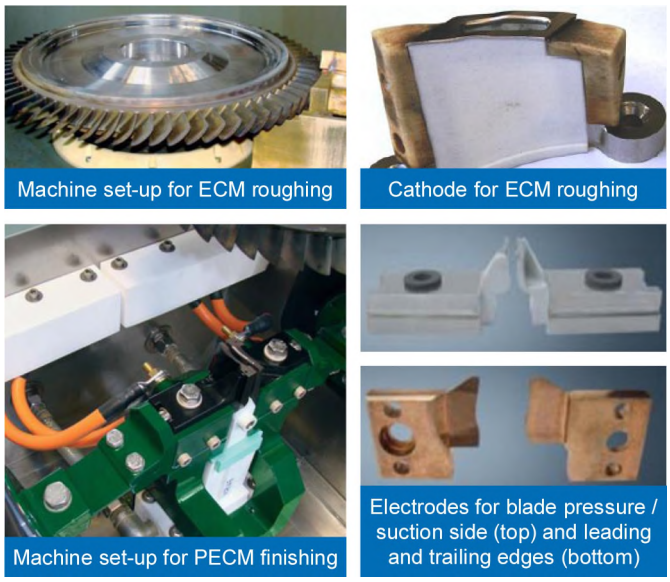


Fig. 20. Machine set-up and electrode design for DC-ECM roughing and PECM finishing of blisk geometries. Based on [55,152].

The machining results for both ECM technologies are presented on the left and middle part of Fig. 21. In order to get a shiny, "hyper-polished" surface, an additional smoothing operation was performed with removal of oxide particles via vibratory polishing with chemical support. Final roughness values were Ra < 0.1 μm and Rz < 1 μm, see right hand photograph in Fig. 21 [152].

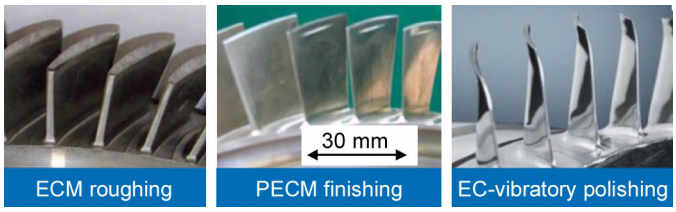


Fig. 21. Production of a nickel-based HP compressor blisk via ECM, PECM and (electro-) chemical supported vibratory polishing, [36,152].

Besides complex blisk geometries, complete turbine wheels for turbo charger applications can also be successfully machined via ECM from solid or from near net shape, see Fig. 22 [72].

3.1.7. EC-machining of cooling holes

ECM technology is also applied in turbomachinery component manufacture for the production of cooling holes. This includes holes both for blades/vanes as well as disks. The major advantages of applying ECM are the production of smooth, stress- and crack-free surfaces. In addition, low contour drilling angles can easily be realised [187]. Fig. 23 shows the EC machining of curved elliptical cooling holes in nickel-based high pressure turbine disks. The long axis of the ellipse has a length of 6.5 mm while the disc has a

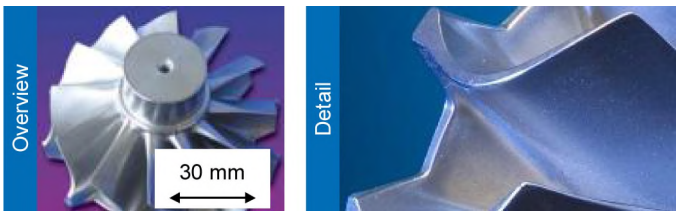


Fig. 22. ECM machining of complex geometries like complete turbine wheels for turbolader charger applications [72].

diameter of 500 mm. The curved design is necessary for an ideal stress distribution during load and cannot be machined via conventional cutting. Both inlet and outlet contours are simultaneously chamfered. The overall machining time for 74 cooling holes amounts to 20 h [83,104].

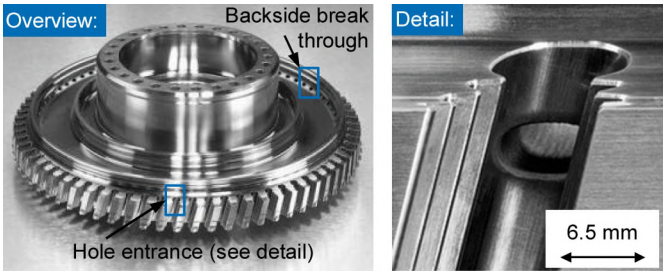


Fig. 23. Machining of curved elliptical cooling holes in nickel-based high pressure turbine disks via ECM, [60,83].

For machining of filigree and high aspect ratio cooling holes in blades, two ECM-based technologies are used in industry. The first process is the Shaped Tube Electrolytic Machining (STEM). The principle is shown in Fig. 24.

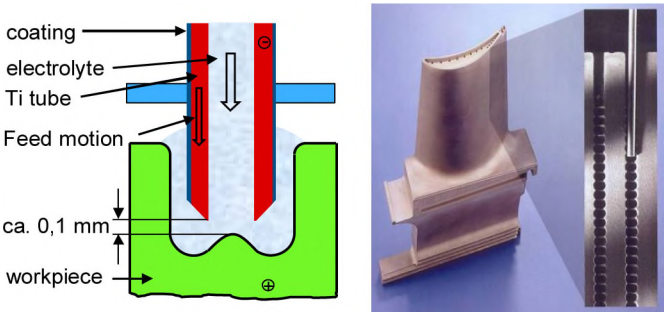


Fig. 24. Principle of conventional STEM and STEM-drilling of turbulated cooling holes via feed rate variation. Based on [62,85].

Because of a side wall insulation of the metallic tubes used as tool electrodes, the machining only takes place in the frontal gap area avoiding side gap widening effects. High aspect ratio holes (up to 600) can therefore be drilled for diameters of 0.3–5 mm. Achievable diameter tolerances are in the range of ±0.03 mm. By using acid based electrolytes like HNO_3 and H_2SO_4, the dissolved workpiece ions are kept in the fluid allowing efficient flushing of the bore holes. Working voltages between 6 and 15 V allow feed rates of up to 4 mm/min. In addition, by periodic reduction of the feed rate, cooling holes with spherical undercuts can be produced. These so called "turbulated" cooling holes achieve a higher degree of efficiency due to the creation of swirls within the air flow [149]. Detailed experimental studies on the influence of process parameters and subsequent process modelling can be found in several publications [4,96,200].

An application example of STEM drilling is shown in Fig. 25. Seven cooling holes per blade are simultaneously drilled in two workpieces within one machine set-up. The drilling length is 70 mm and the diameters range between 0.7 and 1.3 mm [62].

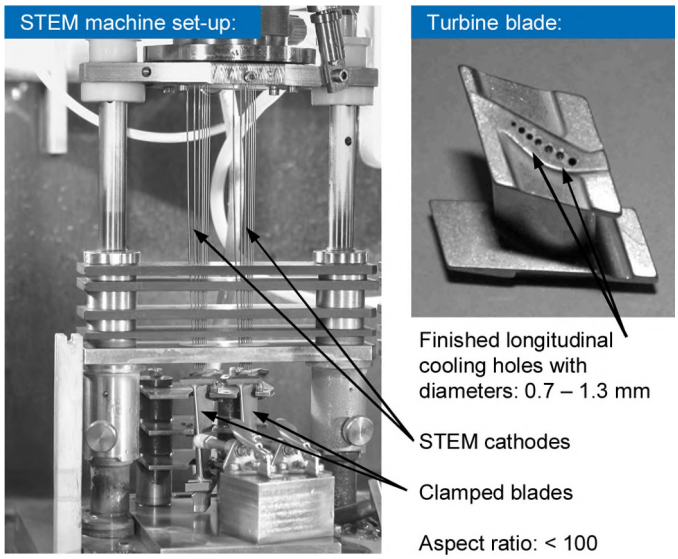


Fig. 25. Machine set-up for STEM drilling of turbine rotor blades and application example [62].

The second high aspect ratio electrochemical drilling method used in aerospace industry is the Electrochemical Fine Drilling (ECF) process, [187]. Its principle and an example of application are shown in Fig. 26.

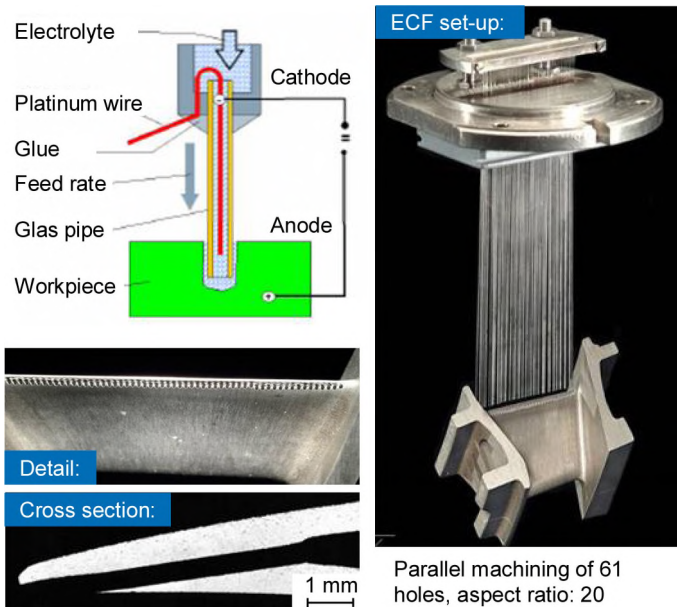


Fig. 26. Electrochemical Fine Drilling (ECF) of cooling holes in nozzle guide vanes – principle and application example [62,187].

ECF utilises stiff glass pipes within guidance systems. Very small diameters down to 0.15 mm with tolerances in the region of ±0.01 mm for aspect ratios up to 600 can be realised. Within the pipe a metallic wire electrode serves as the cathode with working voltages of 60–100 V and feed rates of 1–4 mm/min. Electrolytes such as HNO_3 are used. The example shows the parallel machining of 61 holes with a diameter of 0.5 mm and a drilling depth of about 10 mm within a guide vane (application RB 199). The drilling angle with respect to the workpiece contour amounts to 10° [62,187].

3.1.8. ECM grinding of honeycomb structures

The hybrid process combination of ECM and grinding ECG (see Lauwers et al. [122]) was developed in the 1960s in order to effect efficient burr-free material removal for difficult-to-machine aerospace alloys. The process combination allows the burr-free grinding of turbomachinery honeycomb structures or removal of heat affected zones, see Hascalik and Caydas [79]. The highly complex nature of the process and environmental concerns has led to alternative technologies being developed, limiting the application of this process.

3.1.9. Further research activities and future perspectives

Research activities for ECM drilling of high aspect ratio holes focus on the avoidance of acid handling by using mixed electrolytes and appropriate process parameter adaptations, see [28,185]. Finally, Sen and Shan [171] reported a detailed review on electrochemical macro- to micro-hole drilling processes.

The application of statistical tools (Taguchi method) for the design and optimisation of process parameters during ECM of Inconel 625 was conducted in order to define best electrolyte concentrations, feed rates and working voltages for maximum material removal rates and minimum overcut [39]. Generic aspects of tool design for ECM have been summarised by Westley et al. [208] in order to identify factors such as insulation requirements to improve machining accuracy. The design of appropriate tool electrode feeding paths and trajectory control strategies for complex workpiece geometries such as twisted blade geometries on blisks based on NC-simulation, was introduced in order to avoid interferences, irregularities of machining allowance and short circuits during exit [226,229]. For very thin electrodes which are necessary for narrow slot geometries (e.g. in guide vane segments), tool vibrations due to the high pressure electrolyte flow can arise resulting in poor reproducibility and high risk for short circuits [19].

Specific research on generator development has also been conducted for the electrical pulsed machining of titanium alloys in order to avoid and minimise passivation effects due to the natural oxide film formation, particularly where the change of the electrolyte system to NaCl was insufficient [204]. Similarly, related work focussing on the enhancement of pulse accuracy by MOSFET-based generator improvements has been undertaken [199]. A controlled current rise (up to 600 A/μs) with a special ramp unit allows short pulse durations <20 μs for highest currents [214].

In order to obtain higher material removal rates and best surface integrities both for ECM and PECM technologies, further comprehensive and material specific process adaptations are required. Current R&D work focusses on the detailed process analysis of different electrolyte systems and machining conditions for the machining of γ-TiAl intermetallic alloys with different compositions [42] and nickel-based single-crystalline materials such as LEK94, where the local microstructure and chemical composition of the material are inhomogeneous [33]. Alloying additions with high atomic number, such as W and Re, are preferentially located within the dendrites, whereas Ti and Ta are depleted. Current densities >1 A/mm^2 therefore yield more homogeneous dissolution rates [34]. A high efficiency process for pre-machining/slotting of blisk channels was developed by synchronous motion of simple tool tubes in order to finish 3 gaps simultaneously. To obtain a steady flow condition, the tubes were designed with multi-slit outlets of different width on the outer barrel. The resulting trajectories met the requirements of twisted channels and kept allowances uniform [215].

The broad capabilities of ECM/PECM, when combined in one machine set-up, to achieve both high MRR and good surface integrity together with high productivity is anticipated to see wider use in the future, especially for the machining of new advanced difficult-to-cut alloys. In this context, ECM with plate electrodes moving along the desired contour or even wire-ECM applications (e.g. machining of fir tree profiles on blades/disks) has significant potential for achieving the highest efficiencies, as reflected in its nascent use in industrial applications.

3.2. Electrical discharge machining (EDM)

3.2.1. Introduction

Familiarity with the electrical discharge machining (EDM) process belies the fact that its introduction was relatively recent, machines utilising this mode of material removal appearing only in

the 1950s. For most users, the process entails either die-sink or wire EDM arrangements, which do indeed form the majority of industrial installations however there are a surprising number of alternative machine tool/process configurations that use EDM [88,119,148]. Fig. 27 shows a timeline of technology developments since its inception encompassing fundamental research in addition to innovation and commercialisation.

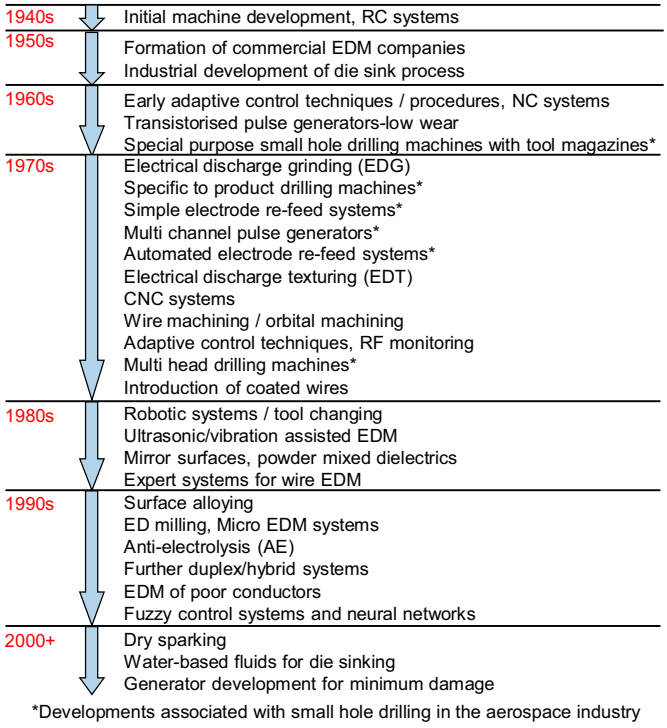


Fig. 27. Timeline of EDM process developments. Based on [8].

Aspects marked with an asterisk relate specifically to key developments associated with EDM small hole drilling in the aerospace industry [189]. Configurations such as electrical discharge grinding (in general a misnomer as the majority of commercial systems involve no abrasive action), have been adopted for superhard (PCD) tool fabrication while texturing systems are used principally for the formatting of rolls in the cold rolling of steel and aluminium sheet/strip, although recent work on texturing allied with surface alloying for fabrication of diffusion bonds in Ti–6Al–4V, has highlighted blisk or blade repair as a possible future application area [17,124,144]. In contrast, dry sparking has yet to see significant application outside the laboratory environment. Since ~2000, the pace of innovation has slowed with incremental rather than step change developments, however it is likely that the introduction of minimum damage generator designs will prove a key milestone in terms of wider Wire-EDM (WEDM) application.

The largest concentration of EDM technology outside general engineering remains in the mould and die industry despite the impact of high speed end/ball end milling in the 1990s. Applications of EDM in turbomachinery manufacture whether for aircraft jet engines or industrial land based gas turbines used for power generation have not changed significantly in the past 40 years. In part, this is due to perceived adverse workpiece surface integrity issues, which are understandably a critical consideration in the aerospace industry where the main tenet and focus is on passenger safety [97]. Received wisdom [137] is such that even today, despite the developments that have taken place in generator technology (see Section 3.2.2), the thermal nature of the EDM process and the resulting workpiece damage, with consequent effects relating to fatigue life and performance, have stifled EDM expansion. Additionally, the development and take-up of laser systems for rapid hole drilling (initially partly dismissed due to shortcomings in accuracy and hole quality), have limited/restricted EDM utilisation. Notwithstanding this, EDM provides better regulation of breakthrough detection/depth control and higher achievable aspect ratios compared to laser systems, [65].

Company specific codes of practice relating to workpiece integrity acceptance standards for the different metallurgical anomalies or surface/subsurface conditions and residual stress states caused by conventional chip forming processes and non-traditional machining processes such as EDM, are operated by all turbomachinery manufacturers, however such information is proprietary and closely monitored. Predictive modelling of workpiece integrity following machining is gathering pace [97] although progress with EDM lags that of turning or milling, as does work involving aerospace alloys as compared to steels. Recent work to predict recast layer thickness/distribution has however shown good correlation with experimental observations when EDM die sinking Inconel 718 [94].

The reasons for choosing EDM over other more conventional processes are that productivity is not limited by the hardness or strength of the workpiece and complex features, or high aspect ratio holes and cavities, can be readily machined. The turbomachinery materials therefore specifically machined by EDM consist of the superalloys Inconel 738, Inconel 939, CMSX4, MAR-M002, MAR-M247, Udimet 720, Nimonic 105, Nimonic 713, etc. The main areas for application include the drilling of cooling holes and die sinking of slots, pockets and grooves (see Section 3.2.3), together with some currently limited wire cutting operations (see Section 3.2.4). Fig. 28 details sample components and ED machined features.

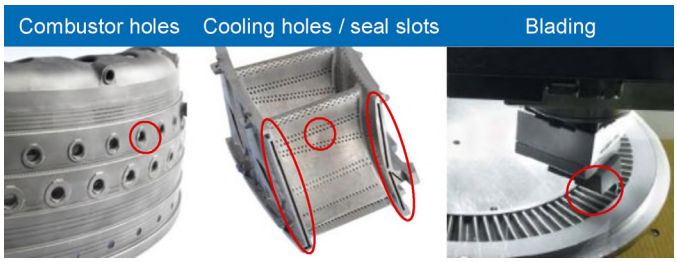


Fig. 28. Sinking-EDM sample turbomachinery features indicated in red (courtesy of Winbro Group, MTU Aero Engines, GF Machine Solutions).

3.2.2. Hardware considerations

The two fundamental configurations that have essentially defined the development of EDM generator technology are relaxation and transistor-based pulse generators. Relaxation generators were the first to be introduced and remained popular due to their simplicity and ability to produce both high and very low pulse energies and discharge durations, making them suitable for roughing and finishing operations as well as accurate precision machining. Conversely, transistor-based systems offered the advantage of programmable pulse shape and greater flexibility in terms of peak current, pulse width and current ignition slope settings, enabling substantial benefits in terms of increased material removal rate, reduced recast layer thickness/heat affected zone depth and application specific workpiece surface quality [9].

Historically, transistor based generators originated from the evolution of relaxation type systems towards controlled-pulse generators, where a separate AC or DC circuit is used to produce high-frequency pulses and control the relaxation-discharge energy independently [170]. For WEDM, removal rates can be increased by producing high current peaks and short pulse durations and special transistor circuits were designed for this purpose in the 1980s using high power MOSFETs. These do not use capacitors but create high current levels by controlling the direction of current supplied to the gap from high power units. For die-sinking EDM, discharge durations are longer than with wire machining which can favour lower electrode wear, but the same principle can be applied to maintain a given current level by alternating current delivery from the power source at high frequency. For finishing sequences, relaxation discharges are commonly employed, as the goal is to

minimise both the peak current and duration of machining sparks. Such high frequency, low energy discharges can also be produced however by controlled-pulse circuits using only transistors, the pulse energy being defined by the gap capacitance.

Modern transistor-based generators use high power MOSFET transistors and ultra-fast recovery diodes for generating peak currents up to 1000 A with durations in the range of microseconds. In order to achieve such performance, state-of-the-art machines have very low line and machining zone inductances below 0.5 μH, allowing rising current slopes up to 600 A/μs. The transistor-based circuits can also be designed to produce trapezoidal pulses for increasing the pulse energy for roughing operations, see Fig. 29. With wire cutting systems, material removal rates on straight cuts with ferrous alloys of up to 600 mm^2/min are possible when employing such configurations. However, triangular pulses with extremely short durations are often preferred in aerospace as they minimise the heat transferred to the work-piece and produce high integrity surfaces devoid of cracks and with reduced tensile stress after finishing operations. For applications involving intermediate roughness (between 0.15 and 0.8 μm Ra), similar results can be achieved with modern capacitor-based generators by exploiting the line to the machining zone as a source of capacitance and as a means for minimising the circuit inductance, thus achieving very high ratios of peak current to pulse width [51]. For polishing operations and micro-machining, very high speed MOSFET and recovery diodes are used for achieving pulse-widths of the order of 30 ns at repetition frequencies of the order of 10 MHz, with peak current values around 1 A [77]. An example of such a circuit is shown in Fig. 30. Under such conditions, surface roughness down to 0.03 μm Ra can be achieved in tungsten carbides and 0.08 μm Ra in steel, with almost zero white layer thicknesses.

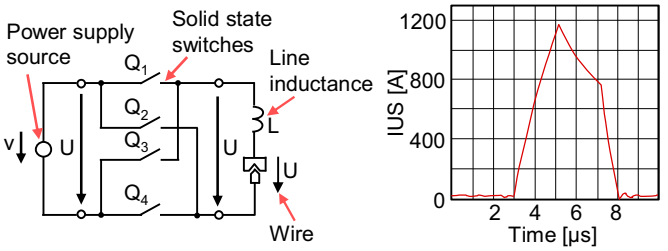


Fig. 29. Basic arrangement of modern transistor-based generator and example of maximum peak current pulse for rough cutting (courtesy of GF Machine Solutions).

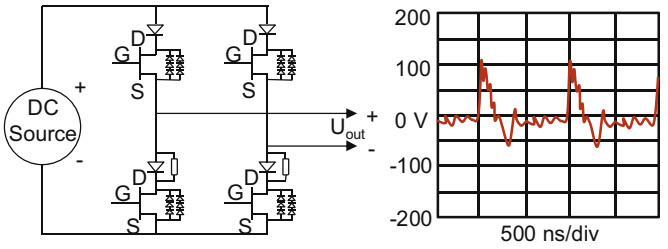


Fig. 30. Principle of generic high frequency anti-electrolysis generator and corresponding sub-μs pulse profile (courtesy GF Machine Solutions).

Other key features of modern generators relate to their ability to tackle corrosion problems by introducing alternative ignition voltages such that the mean value during operation is nil (Fig. 30). Such anti-electrolysis configurations are currently used for the machining of tungsten carbides, steels and Ti-alloys. For die-sinking operations, pulse shape characteristics have not evolved as dramatically as in WEDM, progress being mainly at the process control level involving discrimination of spark quality and effect following signal analysis. Finishing operations have however, reached the same level as in WEDM as both technologies use the same type of hardware for final sequences.

The bulk of EDM machines used for gas turbine manufacture comprise drilling and die sink configurations (estimated ~90%), reflecting the component operations outlined in Section 3.2.1. Wire machines are used but on a limited basis for operations such as blank aerofoil tip machining, however future use for machining blade mounting slots in discs is understood to be under evaluation by a number of leading aerospace manufacturers (see Section 3.2.4). Published evidence for hybrid EDM use in production is slim other than for GE's announcements concerning Blue Arc™ (see Section 3.2.5), and while there appears to be growing academic and related interest in employing vibration assistance as a means to increase EDM productivity. Commercial duplex/combination systems allowing for example the option for EDM drilling and laser ablation in a single machine already exist and are intended for applications such as HP turbine blade and vane machining where laser ablation can be used for removing any thermal barrier coating prior to drilling parent material [209].

Machine tools designed for specific production operations are generally less versatile than their mainstream counterparts but are usually more productive for the particular task at hand. Limited flexibility is however afforded by multi axis CNC capability. An example is shown in Fig. 31, which details an EDM unit designed for machining holes (0.3–3.0 mm diameter, round or shaped/oval) and slots in turbine blades, vanes and segments. Variant models are able to accommodate large annular parts such as combustors and multi hole drilling operations involving up to 45 electrodes (depending on diameter and spacing) operating simultaneously. As with machinery intended for other manufacturing sectors, ancillary equipment/systems for monitoring, probing and inspection are available. In other commercial EDM drilling systems, the combination of an individual tube electrode with a holder and positioning guide in a single assembly, avoids the need to insert the electrode during automatic tool changing, electrode rotation up to 1000 rpm providing improved flushing and removal of debris [143].

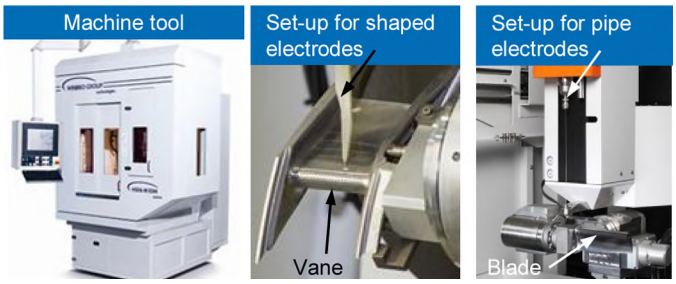


Fig. 31. High speed EDM system and machine set-up for EDM drilling of blades and vanes, (courtesy of Winbro Group, GF Machine Solutions).

3.2.3. ED-drilling/die-sinking EDM (SEDM)

The main areas for research involving die-sink EDM (SEDM) configurations in turbomachinery manufacture are twofold. The first is the machinability/optimisation of electrode type (such as graphite grade) and generator parameters when machining primarily Ti–6Al–4V [80,102,176,203,221] as well as a number of nickel based superalloys including IN 100 [1], MAR-M247 [191], single crystal nozzle guide vane (NGV) alloy C1023 [16] and γ-TiAl [95]. Statistical design techniques are typically employed i.e. Taguchi, central composite designs, etc., when sinking seal slots and similar features with the output measures relating to MRR, electrode wear rate and some aspects of workpiece surface integrity (predominantly surface roughness and recast layer assessment). The second area involves the production of aerofoil blade profiles for impellers and blisks using CNC multi axis milling and electrode feeding strategies with both simple cylindrical electrodes and more complex designs. Here the work relates to development of cutter path strategies, together with bespoke machine and fixturing arrangements [56,131,217]. In contrast, publications on the more fundamental aspects of EDM use with aerospace materials are minimal. An example is the work by Fonda et al. [66] concerning the influence of the thermal and electrical properties of Ti–6Al–4V on EDM productivity, where low duty factors (<10%) are shown to be optimal in order to maximise productivity and workpiece quality.

As outlined in Section 3.2.1, cooling holes, seal slots/grooves, deflector rails, damper grooves and tip recesses on shroudless blades and wedge pockets are the main features machined using EDM, with cooling holes being used extensively on turbine blades, combustors and NGV's in order to ensure adequate gas flow/cooling to enable the engine to operate at higher temperatures and hence more efficiently. Typically holes are machined in rows and groups either singularly or simultaneously with multiple electrodes, and vary in size from 0.3 to 1.0 mm, necessitating electrode diameters as small as ~0.2 mm. Corresponding wall thickness typically varies between 1 and 4 mm. Additionally, diffuser holes may be required with a 3D conical profile at hole entry. Electrode materials are predominantly solid tungsten or brass tubes with both commercial hydrocarbon oils and deionised water being used as the dielectric fluid depending on the machine system employed.

Examples of gas turbine components having features machined by sinking operations are shown in Fig. 32 and include various seal slots in blades and stators as well as wedge pockets on blades. The machine tools used can be more general purpose than for drilling. Electrode materials include copper and graphite ($\leq$10 μm grain size) with the dielectric fluid at present principally hydrocarbon oil (synthetic or mineral), although it is understood that the associated environmental issues are a concern.

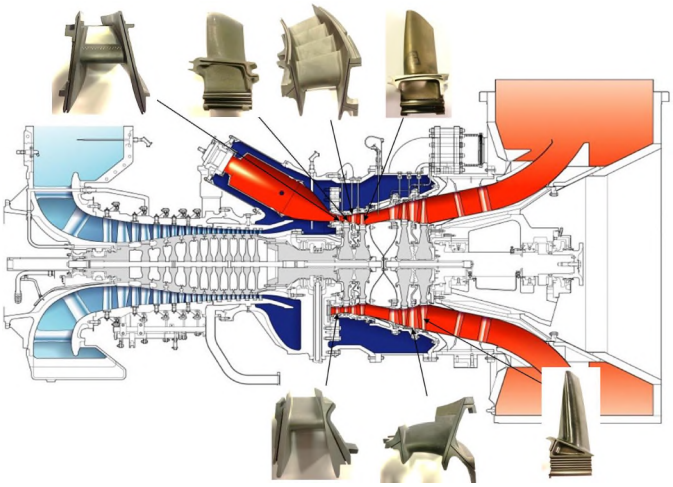


Fig. 32. Industrial gas turbine components machined using EDM (courtesy of Siemens Industrial Turbomachinery).

The general capabilities of SEDM to machine dedicated turbomachinery alloys – in terms of achievable MRR – has recently been analysed at WZL in representative analogy experiments for different geometrical features (Fig. 33). Achievable MRR for constant machine set-up but material specific individually optimised machining of both blisk gaps and seal slots are presented. As basic result it can be concluded that Ni-based alloys generally possess higher maximum MRR during SEDM compared to Ti-based alloys (in contrast to conventional cutting operations).

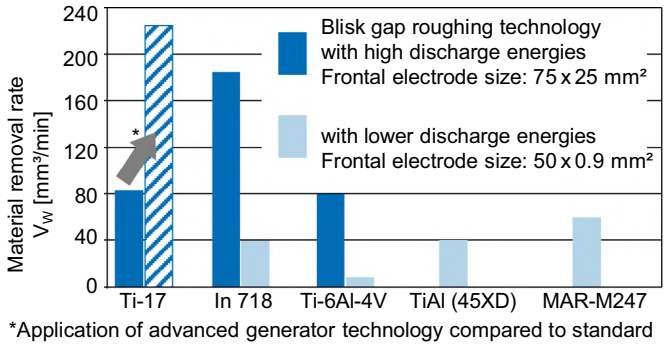


Fig. 33. Typical maximum material removal rates for Ti- and Ni-based alloys during SEDM roughing operations. Based on [113].

In addition, the significant increase of process capabilities in terms of achievable MRR due to latest advanced generator technology improvements are exemplarily detailed for the machining of blisk gaps for Ti-17. Comparing standard Ti-alloys and γ-TiAl it can be stated that during seal slot roughing, considerably higher MRR was achieved for 45XD compared to Ti–6Al–4V. Thus, SEDM – with a high degree of geometrical flexibility – is a viable manufacturing option for future filigree designs of components especially involving new difficult-to-cut alloys.

3.2.4. Wire-EDM

Developed in the late 1960s, WEDM is one of several process configurations where a continuously travelling wire is used instead of a solid tool electrode, for through section cutting of workpieces. Wires are typically uncoated or coated (predominantly zinc based for higher conductivity in the enlarged spark gap) brass, although materials such as molybdenum and tungsten are available where specific properties are required. Without doubt, the largest application area for WEDM is the mould and die industry. Other important markets include the machining of ultra-hard PCD and PCBN cutting tool blanks, biomedical instruments and precision/micro devices.

Unlike conventional ED-die sink/drilling, the use of WEDM for the manufacture of turbomachinery components is currently minimal and confined to either noncritical features or those subject to post processing operations. Established applications essentially include the machining of titanium blisk aerofoil tips, the breakthrough of nickel based superalloy stator vane rings and little else. The reluctance in adopting wider utilisation of WEDM has partly stemmed from slower material removal rates (compared to traditional cutting processes), but more crucially the prevailing perception of poor workpiece surface integrity due to the thermal nature of the process.

Aided by the significant innovations and progress in generator, wire, system control and monitoring capabilities over the last ~15 years, the case for greater uptake of WEDM by the turbomachinery sector is growing, in part prompted by the increased pace of academic/industrial research over the past decade involving nickel based superalloys and titanium alloys. Much of this early work centred largely on the use of statistically designed experiments (Taguchi, response surface methodology) and modelling/optimisation techniques (artificial neural networks, Pareto analysis) to determine preferred operating parameter levels for maximising MRR and improving workpiece surface roughness [84,157,166]. The reported trends with regard to the influence of varying machining conditions on response measures were essentially similar irrespective of the workpiece material assessed. The lack of associated workpiece surface/subsurface integrity results however, prevented any meaningful assessment of process feasibility for turbomachinery components, with experiments generally confined to standard single pass cutting and the resulting surface roughness values >2 μm Ra, well above acceptable tolerances (Ra $\leq$ 0.8 μm) [106].

More recently, research has been carried out to evaluate the potential of WEDM for the manufacture of fir tree or dovetail profiled blade root mounting slots in turbine/compressor discs, see Fig. 34, which are presently finish machined almost exclusively by broaching. While there are relatively few alternatives for finishing slots, several viable options exist when roughing, some of which

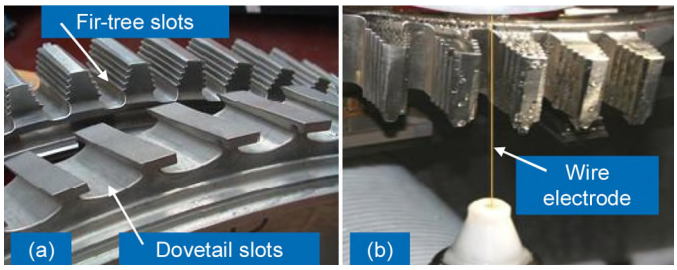


Fig. 34. (a) Sample blade mounting slots profiles in discs and (b) WEDM of fir tree root slot demonstrator [177].

are currently used in production including conventional milling, creep feed grinding (CFG) and abrasive waterjet cutting (AWJC) [48,49]. When finishing, point grinding using small diameter profiled electroplated superabrasive wheels has been extensively evaluated, however the scale of industrial implementation is unknown [15]. The concept of utilising WEDM for producing fir tree root slots was briefly outlined in a paper published in the mid-1980s [47], however there were no indications that the technology was sufficiently mature at the time to be implemented commercially by any of the major aeroengine manufacturers.

Aspinwall et al. [14] reported preliminary experimental work using a high specification 'minimum damage' WEDM machine to investigate the influence of a combined roughing and multiple trim/finishing cut strategy on workpiece surface integrity when machining 10 mm thick Inconel 718 and Ti–6Al–4V material. Discontinuous/non uniform recast layers were observed following the main roughing pass, with average thicknesses in the region of ~6–10 μm for Inconel 718 and Ti–6Al–4V respectively. These were found to decrease steadily with successive trim cuts and near damage free surfaces (essentially zero recast) were produced after 4 finishing passes with workpiece surface roughness between ~0.2 and 0.4 μm Ra achieved after the final trim cut. Analysis of cross sectional micrographs revealed no obvious signs of subsurface microstructural alterations or thermal degradation with minimal variation in microhardness, the low energy high frequency/short duration discharges (>1 MHz for the third and fourth finishing cuts) essentially only removing the damage from preceding cuts without inflicting any additional thermal degradation on the workpiece.

The results stimulated further in-depth research encompassing WEDM of Udimet 720 and Ti–6Al–2Sn–4Zr–6Mo (Ti-6246) aeroengine alloys [9–11,177]. Here workpiece thickness was 30–37 mm, which is representative of typical dimensions in disc root slots. Surface roughness and recast layer thickness following the 4 trim cut strategy did not exceed ~0.5 μm Sa and 2 μm respectively in any of the samples evaluated, the latter being easily removed using a post-etch operation. Residual stress measurements revealed a near neutral state (<90 MPa) at the machined surface for both the Udimet 720 and Ti-6246 specimens following the fourth finishing pass, despite the former being highly tensile (~500 MPa) after roughing. Furthermore, depth profile analysis showed that the tensile residual stresses did not extend beyond ~40–50 μm below the machined surface.

Following modification of generator pulse profiles and manipulation of operating parameters, tests were performed involving a rough and 2 trim cut strategy using both uncoated and zinc coated brass wires in an attempt to improve process productivity [10]. Comparable results were obtained with the updated 2 trim cut procedure, where average recast layer thickness reduced from ~8 μm after roughing to <2 μm in both the Udimet 720 and Ti-6246 workpieces, see Fig. 35. Similarly, surface roughness was maintained at ~0.6 μm Ra while surface residual stress levels were almost neutral (<80 MPa) after the second finishing pass. In addition, significant increases in removal rates were recorded (40% for Udimet 720 and 70% for Ti-6246) when roughing using coated wires over uncoated brass, with no appreciable change to workpiece surface integrity.

As detailed by Jawahir et al. [97], the influence of machining operations on surface integrity and the subsequent knock on effects on fatigue strength/endurance is of paramount importance, especially where safety critical components or those subject to cyclic loading are concerned. In room temperature high cycle fatigue (HCF) tests on rough and finish (using 4 trim cut strategy) wire machined Udimet 720 specimens together with flank milled samples [11], the run-out stress of the rough WEDM specimens after 1.2×10^7 cycles was only 0.39 of the materials ultimate tensile strength (UTS), however the finish specimens recorded a value of 0.59 UTS and the flank milled samples 0.65 UTS, see Fig. 36. The marginal difference in fatigue life between the finish WEDM and milled samples was mainly attributed to the presence of compressive surface residual stress (approx. −220 MPa) in the latter, although the difference was not statistically significant. Complementary trials to assess the effect of finish WEDM on fatigue performance of Ti-6246 samples yielded similar results, see Fig. 36, [177].

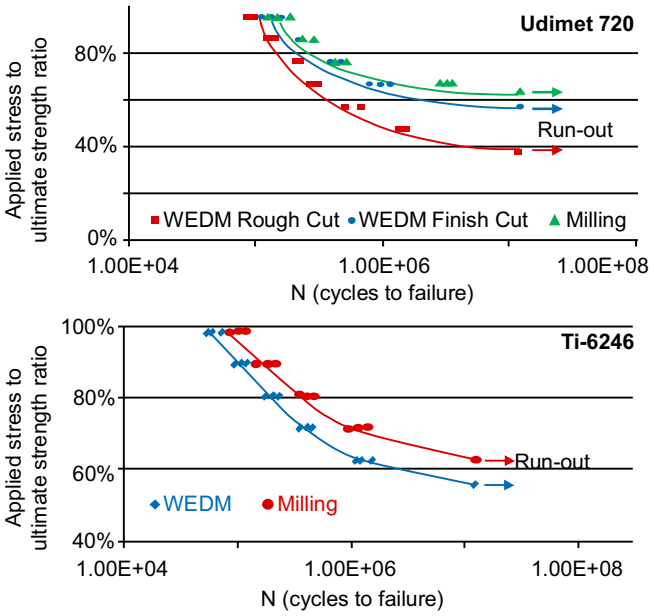


Fig. 36. *S–N* fatigue curves for Udimet 720 and Ti-6246 specimens. Based on [11,177].

Parallel investigations carried out by researchers in Germany [105] to compare the fatigue life of WEDM against ground Ti–6Al–4V surfaces highlighted superior performance in the former. This was somewhat surprising, particularly as associated surface integrity assessment indicated lower surface roughness levels (0.17 vs. 0.25 μm Ra) and a smaller region of heat affected zone (8 vs. 20 μm) in the ground samples. However, high stress concentrations at the edge of sharp cracks observed on the ground surfaces was suggested as the likely reason for the poorer fatigue limit recorded.

In further work by Klocke et al. [106], the reliability and repeatability of a 3 pass WEDM strategy (rough, finish and polish cuts) developed for Inconel 718 was investigated. A series of four fir tree shaped root slots were machined sequentially using uncoated brass wire on a 40 mm thick test block, to mimic a typical turbine/compressor disc section. Cross sectional evaluation of the final cut surfaces (<0.8 μm Ra), showed no evidence of recast layer formation, cracking, porosity, phase transition or microstructural alterations. Precision checks to ascertain accuracy of the machined profile was also performed, with results showing that the cut geometry was within a tolerance band of ±5 μm, see Fig. 37. The mean cutting time per slot however was quoted at ~71 min, which is a relatively slow rate of production compared with alternative processes [113]. Process optimisation (including use of coated wires and modification of generator settings) reduced this value to 40 min, with anticipated potential for further improvement [107]. Associated high cycle fatigue bending (HCFB) tests were carried out by Welling [207] to compare the performance of the optimised WEDM technology against broaching and grinding when machining Inconel 718 samples. Despite higher mean surface roughness values on the WEDM (0.7 μm Ra)

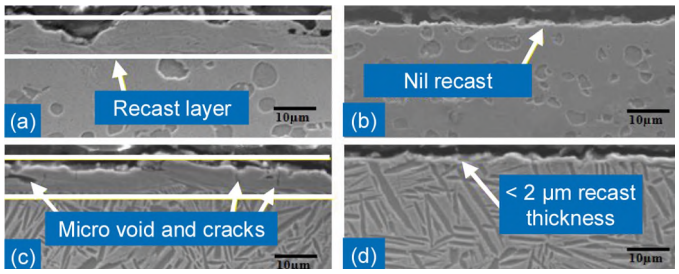


Fig. 35. Cross sectional micrographs for (a) Udimet 720 Rough cut, (b) Udimet 720 Trim Cut 2, (c) Ti6246 Rough Cut, (d) Ti6246 Trim Cut 2 [10].

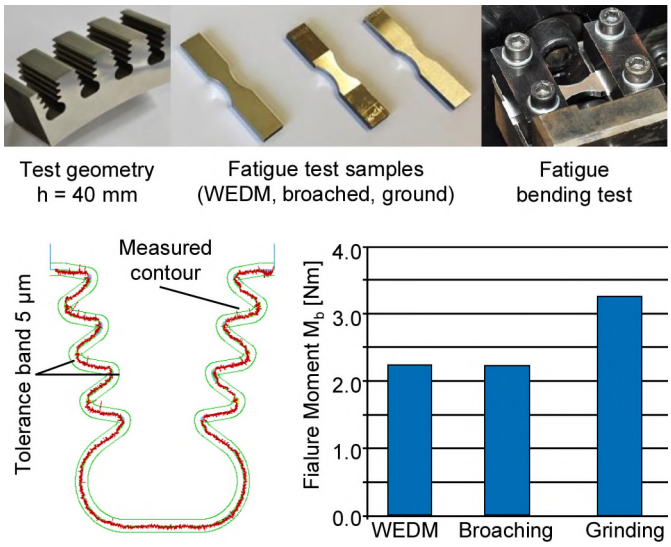


Fig. 37. Precision WEDM machining of fir tree slots and analysis of workpiece functionality via bending fatigue tests, [106,207].

compared to broached (0.28 μm Ra) samples, the failure bending moment was found to be equivalent, see Fig. 37. The fatigue limit of both processes was however ~35% lower with respect to grinding. Not all recent work however has shown damage free surfaces following WEDM [128]. Recast layers ~3.3 μm thick with a roughness Ra of 1.25 μm after 3 trim passes are reported when machining Inconel 718. Other recent research work focusses on the analysis and optimisation of WEDM for Ti–6Al–4V and γ-TiAl [120,167].

3.2.5. Process and machine tool adaptations for specific tasks

The limitations of EDM in terms of material removal rate (MRR) and the dichotomy between attempts at greatly increasing productivity while maintaining or achieving an acceptable workpiece roughness and integrity, are outlined by Wei and his co-authors [205]. These include the fact that with standard EDM systems, pulse mode operation is such that material removal does not occur 100% of the time. Furthermore, an upper boundary exists in relation to the maximum current level that can be usefully applied without compromising process stability, although generator developments over the past decade have enabled ED wire machines to operate with peak currents of 1000 A and slopes of up to 600 A/μs as reported in Section 3.2.2. Even so, with die sink and related drilling operations, excessively high current levels can adversely affect workpiece topography and electrode wear, the associated crater debris producing arcing in the typically narrow inter-electrode gap, and servo instability. Here removal performance is highly dependent on electrode type and geometry, cavity shape and dielectric flushing, and while a stock removal rate of ~1 cm^3/min is possible in steel, for industrial applications involving aerospace materials such as Inconel alloys, removal rates of up to 0.2 cm^3/min (with relative wear below 0.3%) are more realistic.

Improved MRR has been reported with a number of hybrid EDM processes, the most significant relating to erosion systems employing continuous arcing or a combination of controlled arcing and discharges, as a consequence of the higher energy densities that are possible compared with spark discharges alone. Textbook entries relating to electroerosion arcing (as opposed to plasma arcing using a gas assist) as a means to remove material are limited, but where they do occur [137], arc sawing (AS) or less accurately, electrical discharge sawing (EDS), is often detailed involving a thin steel band or rotating disc electrode. However whereas standard EDM uses a dielectric fluid, AS systems generally employ a solution of highly conductive sodium silicate (water glass ~20,000 μS/cm) or alternatively water (~1000 μS/cm) or air, with a DC generator providing a low voltage (6–60 V), high current (200–15000 A) supply. Additionally the feed may be constant/uniform or servo controlled. Workpiece accuracy and roughness are less controllable than for EDM and machined surfaces are subject to greater thermal degradation which can encompass re-deposited material, cracking and a recast layer (typically 50–100 μm but can be greater depending on arcing energy and electrolyte/fluid used), with consequent changes to workpiece microstructure and microhardness.

Commercial machines utilising arcing to rapidly section large forging blanks, honeycomb structures, castings, extrusion products, bar stock, etc., in a range of difficult to cut materials including stainless steels, nickel and titanium alloys, appeared during the 1960s both in the Soviet Union and USA and subsequently in Japan [150]. In contrast to EDM development and growth however, their use was not mainstream or widespread, the main focus of application during the late 1980s and 90s appearing to be in the decommissioning of atomic reactor pressure vessels, where any workpiece damage (typically recast layer material and cracking) and relative inaccuracy resulting from the thermal erosion process, was of little concern.

Reported in several papers on high efficiency electrical erosion, the electro-melting-explosion process outlined schematically by Ye [219], bears some similarity with the AS systems reported above, having voltage and current values when rough processing of 25–28 V and 1600–3000 A respectively, but with the option of fine processing at 1–9 V and 1–90 A. The intended workpieces include nickel and titanium alloys with the preferred working fluid, a low concentration aqueous electrolyte. Gap details during non-contact processing are quoted as 0.01–0.1 mm but with acknowledgement that short duration mechanical contact between the workpiece and rotating tool disc (5–2000 mm in diameter and from 1 to 40 mm thick) may aid processing. Whether the process has been commercialised is unknown. Although limited by modest generator power availability and flushing constraints, AS work reported by Paul et al. [151] was aimed at effecting fast bulk metal removal of nickel based alloy for aeroengine component applications. In contrast to the more familiar cut off operations, the paper details profiling and slotting using 10 mm thick plain and shaped disc electrodes. Workpiece surface integrity evaluation indicated a maximum white layer thickness of 55 μm with cracks propagating to ≤40 μm.

More recent publications cite applications directly relevant to turbomachinery manufacture, in particular the rapid rough machining of aerofoil blades in blisks using high speed electroerosion machining (HSEM/Blue Arc™). Cylindrical electrodes are used with through flushing capability, material removal occurring via transient arcing through an electrolyte, though not one containing sodium silicate, see schematic in Fig. 38. Multi axis tool path movement incorporating dynamic tool wear compensation is employed to 'end mill' the aerofoils with a ball nose tool on a layer by layer basis. The figure shows an example of HSEM blade 'milling' together with sample microstructural damage on Inconel 718. The process is detailed as 15–20 times faster than EDM milling, up to 3 times faster than conventional milling and able to remove upwards of 200 cm^3/min when operated in a pseudo grinding mode with a 25 mm thick rotating disc electrode [205,222].

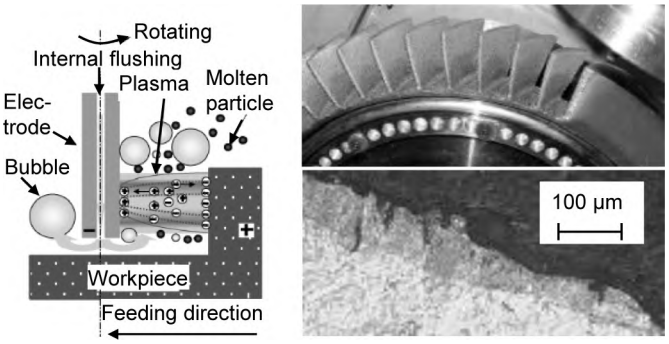


Fig. 38. Schematic of HSEM/Blue Arc™ process mechanism and machining of superalloy blisk (Inconel 718) workpiece [205,222].

The research reported by Zhao et al. [227] on blasting erosion arc machining (BEAM) bears some comparison through its use of either a bundle of graphite tube electrodes (Fig. 39), which can provide a 3D



Fig. 39. Blasting erosion arc machining (BEAM) using bundled graphite electrodes for rough machining of blisk slots. Based on [227].

shaped end face or a laminated electrode with slotted surface and multiple inner holes. In cavity machining of Inconel 718, a material removal rate of 11.3 cm^3/min is quoted for a current of 600 A and an on-time of 2000 μs using transitory/intermittent rather than steady state arcing. A prerequisite for successful operation is the use of high velocity flushing with the water-based dielectric to induce strong hydrodynamic forces into the gap in order to periodically distort and break the plasma column and blast away molten material. Tool wear ratio is detailed as less than 3% with the thickness of the heat affected zone less than 200 μm.

For increasing productivity the simultaneous machining of seal slots in different parts (fairings, panels, etc.) in one machine set-up is state-of-the-art. In addition units for vibration-assisted machining of such slots are under development (Fig. 40).



Fig. 40. Simultaneous machining of several seal slots in one set-up and schematic of twin piezo graphite electrode unit for vibration assisted EDM machining with standard interface. Based on [138,192].

Research involving ultrasonic assisted EDM (USM/EDM) and latterly that relating to lower frequency vibration assisted EDM, has shown there to be significant benefits in drilling/die-sink operations in terms of increased MRR/reduced machining time, increased penetration depth, a reduction in the incidence of arcing together with improvement in sparking efficiency, thinner recast layer and heat affected zone and in some cases reduced tool electrode wear, principally as a result of improved flushing and clearance of debris from the spark gap. In the early 1980s, Kremer et al. [116] in trying to resolve some of the limiting issues of EDM such as poor dielectric circulation and the evacuation of debris and gasses especially with intricate electrodes, showed that using an electrode vibrating at ultrasonic frequency ~20 kHz allowed deeper penetrations and higher feed rates in die sink operations. Feed penetration when using a graphite electrode to machine a steel workpiece increased some 30% when roughing and 300% when finishing. Subsequent publications [117,129,142,186] all involving vibration at ultrasonic frequencies (20–23 kHz) with amplitudes ranging from 3 to 30 μm, both with and without abrasive particles dispersed in the dielectric fluid, detail positive benefits for the USM/EDM approach. The paper by Lin et al. [129] is particularly relevant, the MRR when USM/EDM Ti–6Al–4V with a dispersal of 3 μm SiC in distilled water dielectric (90 g/l) being twice that of conventional EDM. Here the concentration of abrasive is reported as critical, with too much producing unstable discharges. Complementary research with wire machine configurations also detail improvements in performance, Guo et al. [76] reporting cutting efficiency increased by 30% and reductions in both workpiece surface roughness and tensile stress when vibrating the wire at 35 kHz with amplitudes up to 12 μm. Somewhat less striking are the results reported by Han et al. [78] when ultrasonically vibrating a Ti–6Al–4V workpiece (in cutting direction). Here the benefit in MRR compared with standard EDM is quoted as ~10%.

Results for lower frequency longitudinal tool vibration reported by Prihandana et el. [155] and Uhlmann and Domingos [192] are similarly positive, with data for the former when operating at 600 Hz and 0.75 μm amplitude with a 12.5 mm Cu tool electrode, suggesting a 23% increases in MRR and lower workpiece roughness and tool wear rate when machining SS304 stainless steel. In the latter paper, twin piezo-actuators are detailed for the machining of high aspect ratio seal slots in MAR–M247 using graphite electrodes vibrating at up to 1000 Hz with amplitudes from 2 to 16 μm achieving increased MRR and reduced wear.

Further specialised machine equipment has been developed for the flexible machining of radial stator ring cut-outs for blading fixturing with workpiece diameters up to 2000 mm via WEDM (standard precision adequate) (Fig. 41).

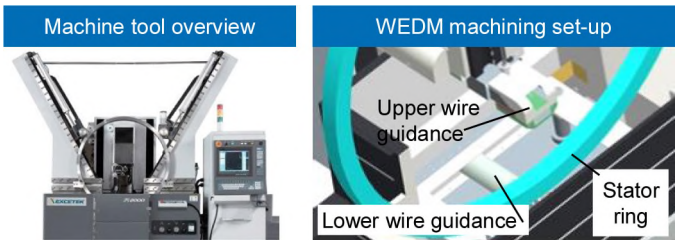


Fig. 41. Machine equipment for flexible machining of blading cut-outs in stator rings, (courtesy of Exetec/Ona Electroerosion).

3.2.6. Outlook and future perspectives

With productivity as a key driver, the move to develop specialised EDM equipment in addition to adapting and optimising standard systems for the manufacture of turbo-machinery components [165] is likely to continue. There is little evidence at present of operating modes such as ED-milling, which is able to utilise simple electrodes, being used in practice, however this may change due to recent developments in hybrid processing, especially where the operation involves only roughing. The considerable volume of data generated in the past 6 years relating to surface integrity and fatigue life, clearly points to WEDM as a potentially viable process to more traditional manufacturing techniques for turbomachinery components. Additional benefits relate to the possibility of 24 h unmanned operation, the flexibility afforded by the software driven process nature in respect of part design changes together with real time condition monitoring procedures. In terms of product miniaturisation, EDM can offer advantages especially for the machining of ceramic components [130,228]. While minimum damage cutting of various nickel and titanium alloys has been demonstrated, producing acceptable surfaces in materials such as γ-TiAl using EDM is more problematic. Poor surface integrity characterised by long/deep cracks which propagate along the grain boundaries into the bulk material as described by Mantle et al. [133] in the late 1990s, remains true, even when using more up to date generator technology with multiple trim cuts.

Despite some six decades of R&D work, current use of controlled electroerosion arcing for turbomachinery manufacture appears extremely limited. Recent work has shown the possibility of significant productivity benefits in specific applications however the lack of process capital/operating cost data, the scarcity of suitable commercial machine tools and the adverse accuracy and workpiece integrity associated with the process need to be addressed for the process to have greater impact.

3.3. Photonic processes I: additive manufacturing

3.3.1. Overview

Additive Manufacturing technologies (AM) enable the build-up of complex objects by the repeated application of thin layers, see Fig. 42. Compared to conventional subtractive processes, economic efficiency is possible with quantities starting from 1, being substantially less dependent on the part geometry. AM originated from the manufacture of prototypes (Rapid Prototyping), but is being increasingly employed for small-scale series production (Rapid Manufacturing)

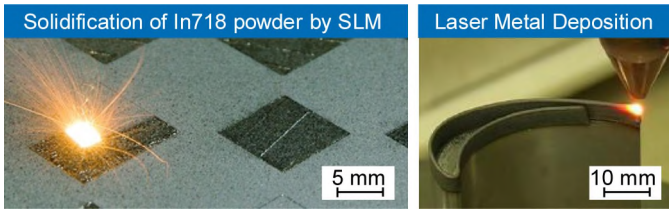


Fig. 42. Additive Manufacturing by Selective Laser Melting SLM [courtesy of IWB] and Laser Metal Deposition LMD [69].

and tooling applications (Rapid Tooling). Deposition procedures are capable of locally applying and solidifying the base material (metallic powder or wire) on a part, rendering this technology extremely efficient for repair applications. In powder bed metal-based procedures, flat layers of base material (i.e. metallic powder) are applied for the complete build area. In a second step the current part cross section is solidified by selected heat input through laser beam melting (commonly called selective laser melting - SLM) or electron beam melting (EBM). The principal limitations of the approach include the requirement for additional support structures to ensure proper heat dissipation and to reduce distortions. Build-up of overhanging structures therefore requires advanced process knowledge and is followed by additional post treatment steps. The basic process mechanism is detailed in a paper by Kruth et al. [118]. Development of AM for aeroengine and turbomachinery production started in the 1990s [212]. Besides prototyping, tooling and jig applications, the direct manufacturing of serial parts is of major interest due to increased deposition rates as well as improved material properties [210]. Volume build rates of up to 10 cm^3/min for Inconel 718 are feasible in layer-wise laser cladding AM [69,211]. To overcome admission restrictions especially in the aerospace sector, a great deal of effort has been put into qualification [223], testing and certification of additively manufactured parts including development of online quality assurance systems [45].

The additive manufacturing technologies, see turbomachinery examples in Fig. 43, offer new possibilities for product design (complex shapes, hollow spaces, undercuts) while simultaneously allowing for a significant cost and weight reduction [160]. MTU Aero Engines is using AM for a wide range of parts, e.g. vane segments and honeycomb structures for rigs and "ground only" engines [82]. The production of the first flying component, a boroscope eye for the PW1133G NEO started in 2013 [121].

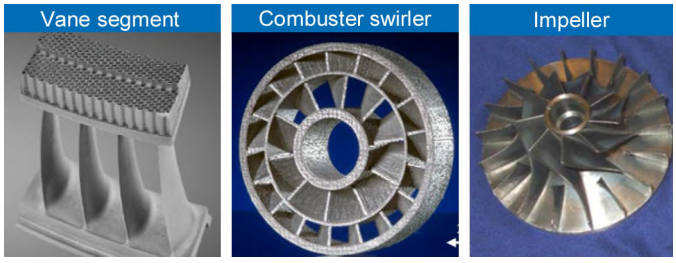


Fig. 43. AM manufactured vane segment with honeycomb seal structure [54], functional prototype of In 718 combuster swirler [103] and In 718 impeller blading build on pre-machined part [216].

General Electric (GE) Aviation is also moving towards serial production and recently announced the manufacture of a leading edge for blades and a fuel injector in 2013 [213]. By 2020, GE is scheduled to produce more than 100,000 additively manufactured components for its LEAP and GE9x engines. Of major interest is a design optimised fuel nozzle, which is ~25% lighter and five times more durable than conventionally manufactured fuel nozzles [71]. NASA uses additive technologies to build various parts of space launch systems and considers Selective Laser Melting (SLM) to be the manufacturing future [92].

3.3.2. Future applications

AM is expected to have considerable potential due to increased design opportunities that include graded workpiece properties

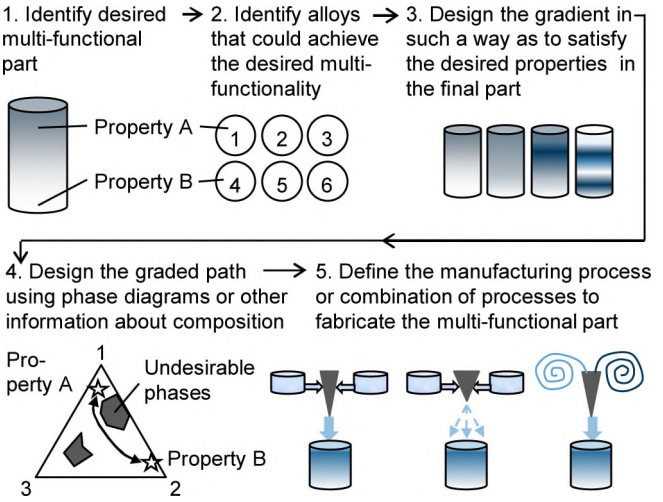


Fig. 44. Method for fabricating gradient alloy parts with multi-functional properties. Based on [230].

(see Fig. 44), organic shapes or geodesic structures during the manufacture of diverse turbomachinery components (blades, vanes, shrouds and according segments, blisks, casings, tubes and brackets, nozzles, liners, etc.) [3,6].

As an example for future application, a new approach to compressor casing design was discussed [12]. Here, auxetic structures (i.e. materials with negative Poisson's ratio) are used to reduce the relative tip clearance by adapting the behaviour of the casing to that of the rotor, see Fig. 45. The reduction of relative tip clearance resulted in an increase in compressor efficiency. Due to the fact that the fabrication of auxetic structures is difficult or even impossible with conventional manufacturing techniques, the application of additive manufacturing technologies (SLM or EBM) is proposed. The design freedom provided by additive manufacturing can in the future be used for the fabrication of hollow rotor blades resulting in a decrease of total engine weight. Furthermore, the variation of wall thicknesses makes it possible to shift certain blade eigenmodes in order to reduce the total vibrational load.

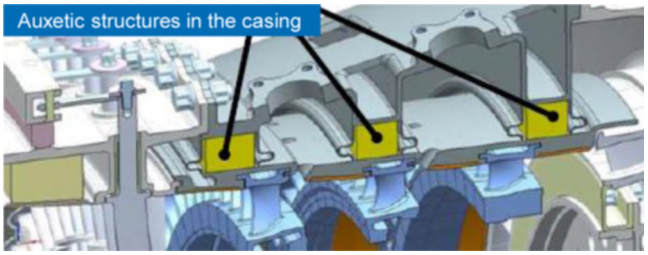


Fig. 45. Position of the auxetic structures in a double-walled split casing for reducing the relative tip clearance. Based on [12].

3.3.3. Process development

Additive processing of Ni- and Ti-based alloys used in turbomachinery applications is mainly done via SLM or EBM. In laser processing, the absorption of a high intensity near infrared (NIR) beam causes the metallic powder particles to melt and form a continuous bond between subsequent scan tracks while cooling down from melt temperature. Absorption is dominated by multiple reflections at individual powder particles, which makes the absorption of NIR laser beams in powder layers significantly more efficient than for bulk material. In SLM, an inert gas flow at slightly over pressure is used to prevent oxidation and to remove sputter particles ejected from the process zone. The solidification mechanisms [118] are controlled by the melt flow behaviour and wettability and can be varied by the applied scanning strategy. Since focal diameter, powder grain size and layer thickness are of the same order of magnitude, filigree turbomachinery components can be fabricated to precision of 100 μm with commercially available system technology.

During solidification the size of the melt pool is mainly determined by the heat conduction through the solid because the thermal conductivity of the surrounding metallic powder is substantially lower [5]. In case of insufficient contact between adjacent layers, process instabilities may develop causing the ejection of melt droplets and sputter particles [135]. The melt's temperature may rise significantly above the evaporation limit during material exposure and a plasma plume is formed which exerts a recoil pressure on the melt pool and increases the sputter activity [139].

Compared to a clear focus on high temperature Ni-base, Au- and steel materials, EBM technology developed by ARCAM AB has centred mainly on titanium alloys. Zäh and Lutzmann [224] modelled the EBM process and developed understanding of the "powder blowing" effect caused by electric charging of the powder particles. The technique requires a low-pressure vacuum or inert gas atmosphere (10–1 Pa) in the processing chamber to reduce electrical charging of the surrounding powder bed [75]. By using preheating strategies, it is possible to process materials susceptible to cracking. Preheating temperatures of up to 800 °C [173] are possible, enabling the reduction of support structures through reduced thermal gradients. Additionally, using a split electron beam (the so-called multi-beam strategy) allows for high speed processing compared to conventional hatching strategies used in SLM. The current system technology development in both cases focuses on high power beam sources and multiple scanning units to enable the processing of materials with low absorbance and high thermal conductivity (i.e. Cu). Advanced exposure strategies subdivide the component into skin and core areas in order to use different process parameters. The skin section is usually solidified with moderate energy input and small focal diameters to account for filigree structures and optimised surface properties, whereas the core is exposed to high energy input and big focal diameters to increase the manufacturing speed. High power SLM with tailored process control (skin-core) allows Inconel 718 components with relatively low thermal conductivity ($\lambda \leq 30$ W/mK) to be manufactured with a density $\geq$99.5%. Hence, the use of lasers with output power of up to 1 kW enables build-up rates to be increased by a factor of 4, compared to conventional SLM [136]. Advanced process and cooling strategies have also been developed for the machining of complex blisk parts [211], with typical examples shown in Fig. 46.

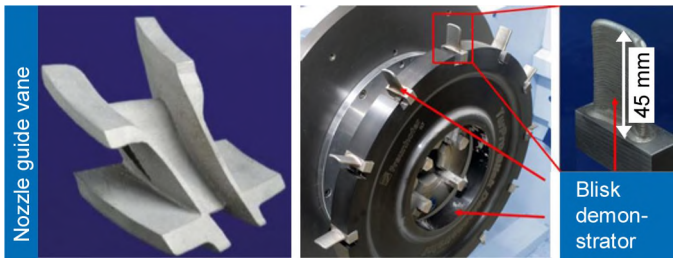


Fig. 46. IN718 Nozzle Guide Vane studied for application of High-Power SLM [Courtesy of TurboMecca/136] and blisk demonstrator used for AM machining and cooling strategy development [211].

In many cases, EBM and SLM technologies do not fulfil requirements relating to surface quality or dimensional accuracy [44], and post processing by means of conventional machining or sandblasting becomes necessary (see Section 3.3.7). Current research activities focus on the optimisation of exposure parameters and on statistical confirmation of material properties. It was shown that comparable part quality can be obtained when moving towards higher layer thicknesses thereby increasing economic efficiency [115]. Further research activities centre on the application of multiple materials in the same process to enable functional coatings or geometry adjusted material properties. By using laser cladding (see Section 3.3.6), the combination of different materials to produce functionally graded parts was proven to be feasible for Ni-base alloys and Ti-based alloys by Domack and Baughman [58]. With SLM, the manufacture of metallurgically bonded joints between WC/Co and steel for use in tool construction has been demonstrated [146,183]. Functionally graded zirconia Ni-based alloy parts on Waspaloy substrates have successfully been built [140]. Here, the mass fraction of Zr in the powder mixture increases layer by layer with build height. This layer-wise change of powder composition limits graded material transitions in one direction. By using selective coating mechanisms, it is also possible to create functionally graded materials in any desired orientation [146,147].

3.3.4. Mechanical properties and microstructure

The mechanical properties and microstructural features of additively manufactured components are governed by the high cooling rates during the solidification process, normally resulting in small grain sizes. Since Inconel 718 is an age-hardenable austenitic material, its strength is largely dependent on the precipitation of the γ'-phase. By appropriate heat treatments, the mechanical strength becomes comparable to wrought material.

In the as-fabricated form, the material has non-isotropic strength and strain properties. Upon hot isostatic pressing the microidentation hardness (HV) can be increased to approximately 6 GPa while the recrystallization can reach up to 10 vol% [7]. The precipitation strengthening of γ' and γ'' and the inter-crystalline strengthening of needle-like γ-phase at the grain boundaries are the main reasons for the high micro-hardness values seen in the Inconel 718 samples fabricated by SLM and post age-hardening treatment [201]. The level of microstructural defects (porosity, junction errors, etc.) can be decreased by moving towards higher energy inputs (lower layer thickness, lower scanning speed and higher laser power) and is typically in the order of 0.01%. Additionally, advanced technologies such as Selective Laser Erosion and Laser Remelting to improve surface integrity are under development [218].

The right hand photograph in Fig. 47 shows that the microstructure of Ti–6Al–4V processed by laser-based additive manufacturing is mainly composed of acicular martensite (α' phase). While the yield stress and the ultimate tensile strength are relatively high, the ductility can be considered as low (<10%). Post-process heat treatment can improve the mechanical properties of the material by changing the microstructure and reduce thermally induced residual stresses in the built part. Due to the fact that the resulting microstructure differs significantly from bulk Ti–6Al–4V alloy, other heat treatment parameters compared to forged or cast Ti–6Al–4V are necessary [197].

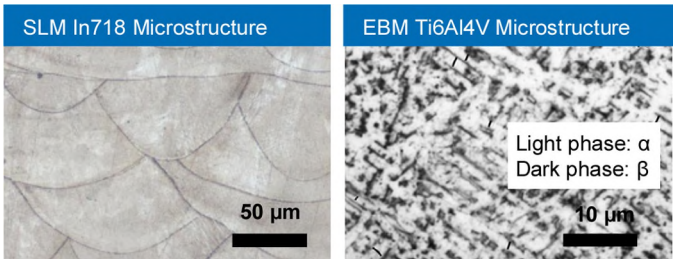


Fig. 47. Microstructure of as-fabricated In718 showing consolidation structure (courtesy of IWB) and of EBM-processed Ti6Al4V [90].

Electron beam melted Ti–6Al–4V exhibits anisotropic behaviour of its mechanical properties according to studies performed by Hrabe and Quinn [90,91]. Elongation in the vertical direction (parallel to the electron beam) is detailed as ~30% lower than is the case for horizontally oriented parts. In contrast to classical annealing where the microstructure is typically discrete α in continuous β, the microstructure obtained by EBM was found to be continuous α with discrete β.

Other materials like TiAl are also of interest for future jet engine applications because of their low mass compared to nickel-based alloys. While EBM produces parts with a relative density of approximately 98% (above 99% after hot isostatic pressing), TiAl components manufactured with SLM show poor mechanical properties and a relative density of ~97% due to cracks [197]. For Ti–6Al–4V densities up to 99.98% can even be achieved

as-built. Further microstructural analysis of standard as well as advanced alloys such as Ti–6Al–4V [41,220], Inconel 718 [184], Rene41 [127] and TiAl [141] are detailed in several publications.

3.3.5. Quality methods

Currently, post-build inspection procedures account for as much as 25% of the time required to produce an additive manufactured engine component. However, by conducting inspection procedures during component build-up, a significant acceleration of production rates is expected [70]. Common post-build quality methods in aeroengine applications include, among others, the verification of part geometry through noncontact optical measurements. Since geometrical accuracy is crucial for functionality, a great deal of effort has been put into reliable determination of the entire external geometry. Testing for inner defects is done through well-established non-destructive methods like X-ray or ultrasonic inspection.

Taking advantage of the layer-wise build up procedure in additive manufacturing, online monitoring can provide complete part inspection during manufacturing. The principal approaches can be divided into coaxial setups sensing the process emissions directly at the current beam position with off-axis setups usually monitoring the complete build substrate at regular intervals.

A coaxial setup, which focuses on monitoring the irradiance emitted by the melt pool was developed by KU Leuven [46]. Since the system uses the same scanning unit for material processing and process monitoring, the detector elements are always focused on the current process zone. The total melt pool area is identified to be the relevant detection variable when analyzing process irregularities. With regard to real-time process control, commercial implementation of this system working in the kHz range is currently under development [23]. The usable wavelength band is however severely restricted to a small band around the laser wavelength because the same optics have to be employed.

The feasibility of layer-wise process monitoring based on a microbolometer IR-camera is shown for SLM by Krauss et al. [114]. Deviations in the laser melting process, occurring at a timescale of several tens of milliseconds can be detected by evaluation of properties of the heat affected zone under idealised conditions. Thermographic process surveillance, see Fig. 48, is particularly well suited for investigating the heat balance and geometry dependent heat accumulation resulting in inhomogeneous material properties and residual stresses. In this regard, the understanding of mechanisms of heat regulation [225] is of fundamental importance. For the EBM process, an IR camera based approach has been developed [162,169] focusing on the flaw detection directly after layer solidification. To overcome the shortcoming of not being able to monitor the actual solidification process due to metallization effects, Dinwiddie et al. [57] analysed different materials for use as a continuously rolling window for the EBM process. Further process monitoring approaches are detailed in several other publications [27,40].

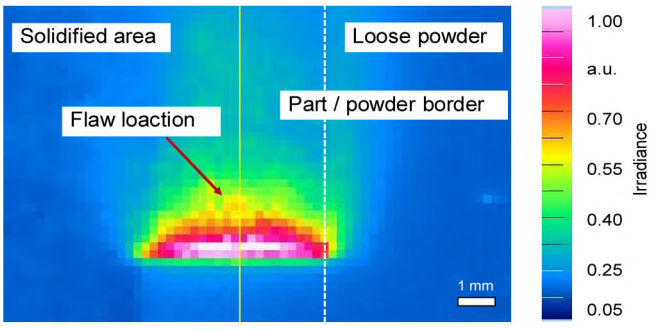


Fig. 48. Thermogram of the heat affected zone after passing of an artificial flaw during SLM [114].

3.3.6. Repair cladding

The efficiency of machinery is directly dependent on the degree of wear and/or erosion, which is an unavoidable result of usage. Worn turbine blades can affect the whole performance of the system and cause a reduction of the turbine efficiency producing high energy losses. Even minor damage on the tips of turbine blades can have major implications. In order to maintain a high performance level, excessively worn turbine blades are either replaced or repaired. As these turbomachinery components are made of high quality and therefore expensive Ni- or Ti-based alloys [156], the repair of these parts is often first choice.

Laser cladding by powder injection is one possible technology to restore for example the tips of worn turbine blades. Such laser based technology is known by various names e.g. laser metal deposition (LMD), laser engineered net shaping (LENSTM) or direct metal deposition (DMDTM). The LENSTM technology was developed at the Sandia National Laboratories in 1995 [126]. By focussing a high power solid-state laser (in general fibre or disc laser) onto a metal surface, a melt pool evolves as a consequence of absorbed laser light. From a powder nozzle that is either attached laterally or coaxially to the focussing optics, metal powder is injected into the melt pool. This instantly changes to a liquid phase after reaching the melting temperature. Because of the moving laser focus, a movement that is determined by the feed direction and feeding speed, the liquid metal re-solidifies and as a result a weld track evolves on the workpiece surface. For protection and transport, a chemical non-reactive inert gas such as argon or helium is applied to prevent oxidation of the metal powder during the melting process. A detailed description of the laser metal deposition process and system technology can be found in several texts [132,190]. In Fig. 49, a schematic of the basic process setup of laser cladding by powder injection and an application example involving edge repair is displayed.

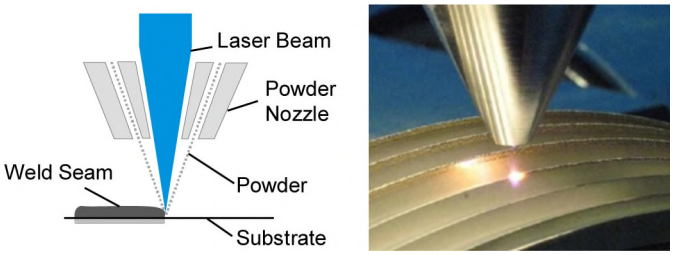


Fig. 49. Basic setup of the laser metal deposition (LMD) process, based on [18] and example of application during edge repair [69].

As described previously, LMD is an economical and highly flexible repair technique which is already applied in the turbomachinery industry [26], for example to build-up worn tips of turbine blades and labyrinth seals [18,161], see Fig. 50. Further examples are the reconditioning of groove walls on HPC front drums made of Ti–6Al–4V and Ti-6246 or the repair of flanges on HPT produced with Nimonic PE16 with Inconel 625 powder. Due to the minimal heat input from the LMD repair process, distortion of the component was almost completely avoided [103]. Process adaptations have been developed especially for the repair of Ni-based superalloys with high Ti/Al composition in order to reduce cracking susceptibility [26]. For the repair of aeroengine components the Fraunhofer ILT in Germany for example has already been

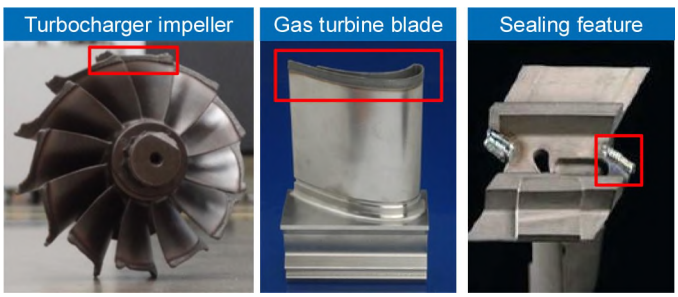


Fig. 50. Blading repair (red boxes) with laser cladding: Turbocharger impeller [99], gas turbine blade [69] and labyrinth seal features [159].

successfully certified by Rolls-Royce Deutschland for 15 different repair applications [68].

In general, different approaches are possible for the repair of worn turbine blades, however coaxial powder nozzles have proved to be more suitable for this task than lateral arrangements [182]. The major disadvantage of a laterally positioned nozzle is the fact that the three-dimensional free moving space is limited and hence, the flexibility of the process is reduced. Furthermore, the quality of the welding tracks produced with lateral nozzles strongly depends on the feeding rate direction, whereas those fabricated by applying a coaxial powder nozzle are not directly influenced by the feeding rate direction.

Although coaxial powder nozzles are well-established in the field of turbine blade repair, powder efficiency falls behind that of a lateral powder nozzle [182]. As the materials of a turbine blade are precious, different approaches have been developed to increase the powder efficiency of the repair process. For example copper moulds in which the tip of the blade is re-built up are used [182]. Here, not only material waste can be avoided but also the required time for post-processing such as machining can be significantly reduced. Furthermore, the time for the repair process can be decreased by applying special optics. In order to produce weld seams of an aerofoil, laser focusing optics (generally referred to as Zoom optics) that can dynamically change the focus diameter during the process have been developed.

The laser cladding process is also an established technique for coating applications. It has been used to generate wear-resistant coatings on the shroud shelves of turbine engine blades in order to increase the wear resistance and lifetime of these components [174]. Additionally, resistance against wear of certain part sections can be achieved with hard-facing by the use of laser cladding [159]. In this context ceramic materials such as zirconium are applied to deposit a wear resistant protective layer.

3.3.7. Post processing and finishing of AM components

In laser cladding additive manufacturing, only near net shape structures can be generated or restored, meaning that post-processing, primary milling to achieve the desired surface quality and the final part geometry is always required. Hence, the combination of laser cladding and machining is part of current research activities. For example since 2008, a UK based consortium has been developing a combined approach known as the "Remanufacture of high value products using a combined Laser cladding, Inspection and Machining (RECLAIM)" system [99]. Within the Fraunhofer Innovation Cluster "TurPro – Integrative Produktionstechnik für energieeffiziente Turbomaschinen" in Germany, similar repair as well as new part production process chains have been developed including a complete CAx framework approach [69]. Fig. 51 shows typical examples of subsequent post processing of AM manufactured parts in order to achieve the final functional macro and micro workpiece geometry. Additionally, ECM technologies are also gaining interest as an alternative to conventional cutting and/or polishing or blasting operations.

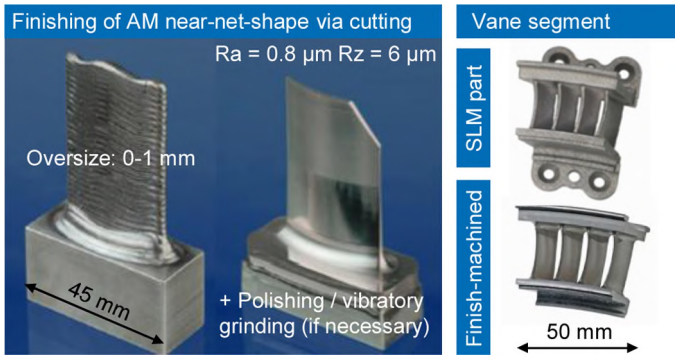


Fig. 51. Examples for subsequent post processing of functional surfaces on AM manufactured components: Near-net-shape HPC In718 blade mock-up [69] and nickel-based vane segment [159].

3.4. Photonic processes II: laser drilling of cooling holes

3.4.1. Introduction

Approximately 5% of all industrial laser material processing applications are laser drilling operations [25]. In this context, the generation of cooling holes in gas turbines for aircraft as well as for power plants is one of the most important, established drilling applications. The steady progression of laser-based system technology (e.g. laser sources, data preparation software, machine control, positioning system, sensor devices, etc.) and the development of novel laser drilling strategies, offering design freedom together with its cost effectiveness has increased significantly during the last decade. Assuming that suitable technology for industrial series production is available, it is possible to drill hundreds/thousands of cooling holes with high precision and of variable diameter and shape in multi-material blades of complex geometry, see Fig. 52.

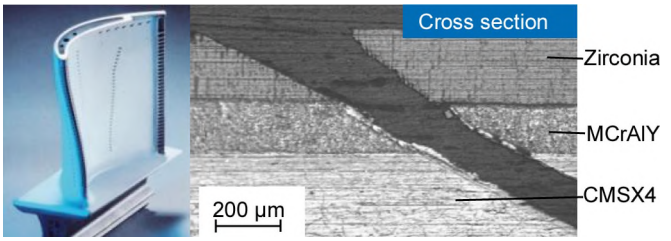


Fig. 52. Laser drilling of cooling holes: Nickel-based turbine blade coated with a ceramic wear resistance layer with cooling holes [25] and cross-section of a cooling hole drilled in a CMSX-4 turbine blade coated with a MCrAlY and zirconia wear resistance layer [89].

One of the main challenges is drilling through multi-layer material systems composed of metal coatings with at least one ceramic wear protection layer without enhanced formation of micro-cracks and thermal induced damage causing a removal of the coating layers. Furthermore, to achieve significant cooling performance the cooling holes are generally tapered or shaped.

3.4.2. Theoretical background

In general pulsed laser systems are applied for laser drilling processes, where selection of the pulse duration depends on the hole characteristics and the material being processed. In the field of laser drilling of turbine components, pulse duration is normally of the order of nano- or milliseconds. The required pulse energy basically depends on the exact chemical composition of the material, the material thickness and the desired hole diameter and shape. In this context an increase of pulse energy generally causes higher drilling rates, but a decrease of drilling quality such as enhanced formation of melting deposits on the workpiece surface and hole edges.

The fundamental interaction mechanisms during laser drilling are schematically illustrated in Fig. 53. A detailed explanation of the different physical mechanisms is detailed by Poprawe [153]. Different physical mechanisms take place inside the irradiated material volume depending on laser pulse duration and laser pulse

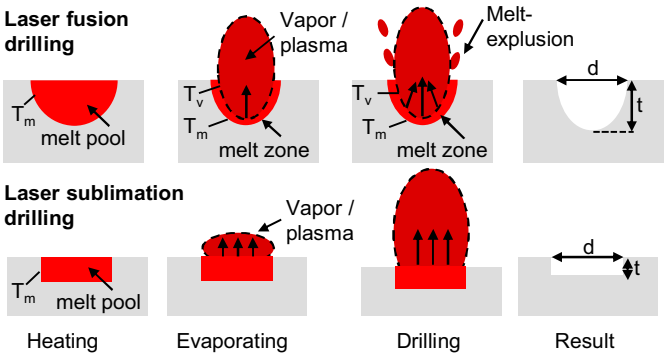


Fig. 53. Physical interaction mechanisms during laser fusion drilling and laser sublimation drilling. Based on [153].

peak intensity. The dominating effects causing material removal are melting and vaporisation. Assuming a temporal and spatial Gaussian intensity distribution of the incoming pulsed laser beam, vaporisation occurs in the hole-centre and melting in surrounding material sections. For a laser peak intensity of approximately 10^6 W/cm^2 and pulse durations of the order of several milliseconds, melting is the dominating effect being responsible for material removal and hole formation.

Initially, the irradiated material is heated up to its melting temperature and a significant melt pool evolves. As a consequence of further energy input vaporisation occurs. Along the drilling axis a dense vapour plume is formed that cannot pass the molten material. Due to recoil of the vapour plume, the melting at the bottom of the hole is continually accelerated and the molten metallic material is expelled along the hole edges. The expulsion of molten vapour material is assisted by applying an inert gas process-stream. Although typically coexisting with vaporisation, the dominating effect is melting and the process causing material removal is melt expulsion. In this context, the drilling process is denoted as fusion or heat drilling. As a consequence of melting, expulsion of small re-solidified particles remain at the hole edges. To achieve typical cooling hole depths of between 8 and 25 mm, a sequence of several laser pulses are required. Furthermore, additional post-irradiation is necessary to remove the re-solidified particles from the edges of the holes and to achieve improved hole quality.

With a further increase of laser peak intensity greater than 10^6 W/cm^2, sublimation drilling occurs. In this case, the dominating effect causing material removal is ablation by vaporising plasma formation. In this context, the applied peak intensity has to exceed a material-dependent threshold value. To achieve such high intensities, shorter laser pulses are required. A system suitable for sublimation-drilling is a Q-switched Nd:YAG laser with pulse durations of the order of 10–100 ns. A detailed explanation of plasma formation and resulting material removal can be found in the literature [132,153].

3.4.3. Drilling operations

Industrially established laser drilling operations include single-pulse drilling, percussion drilling, trepanning and helical drilling. For cooling holes in turbine blades the relevant drilling operations are percussion drilling and trepanning [25]. Furthermore, there exist different approaches to drilling holes of complex shape and varying diameters by combining both. The principles of trepanning and percussion drilling are schematically shown in Fig. 54. A detailed theoretical description of the drilling technologies is presented by Poprawe [153] and Majundar [132]. During the drilling process, an inert process gas stream protects the focusing optics. The gas stream is also employed to assist material removal and to prevent oxidation and necking of the holes by melting deposits from ablated material.

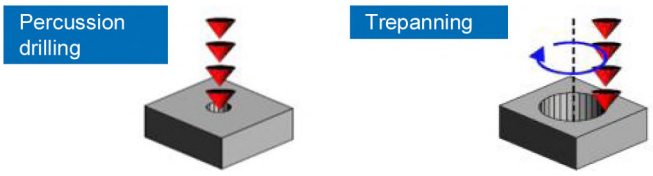


Fig. 54. Principle of percussion drilling and trepanning, [52].

During percussion drilling the laser spot is stationary at the same position on the workpiece in contrast to the trepanning operation. The diameters of the approximately cylindrical holes are commonly of the order 0.5–0.7 mm and the achievable aspect ratio is in the best case 1:20 [25]. An important point is the exact positioning of the focus plane relative to the workpiece surface, which is a function of the required results and workpiece material, the optimal position of the focus spot being located approximately 5–15% of the workpiece thickness under the workpiece surface [25]. In practice the best setting for a specific problem will be empirically identified by analysing hole quality in terms of geometry, distribution of cracks and the amount of ablated material recombining at the hole edges and on the workpiece surface [125].

When trepanning, the laser beam is rotated relative to the workpiece, whereby the laser spot diameter is distinctly smaller than the diameter of the hole. A hole is generated by removing a cylindrical core during one circulation of the focused laser beam. Technically speaking trepanning is a laser-based hybrid process involving classical drilling and laser cutting. Additionally during laser spot circulation, the angle of incidence on the workpiece surface can be varied by influencing the taper angle of the drilled hole [24]. Tilting the focused laser beam is realised by an arrangement of rotating optical components, for example a dove prism with a defined beam displacement at the entrance of the optical element, or by means of tilting reflective optics [24]. The principle of a rotating laser spot provides the opportunity to generate holes with high reproducibility and high flexibility in terms of the hole design. For instance, the hole diameter is not directly related to the laser spot diameter as is the case for percussion drilling. Furthermore hole shape can be non-circular. In comparison to percussion drilling, trepanning is more time-consuming and the heat input into the turbine blade is larger.

3.4.4. Generation of complex cooling holes via process combination

Two types of cooling holes are used for turbine blades, one shaped like conical nozzles the other cylindrical holes where only the exits possess a conical shape. This latter type affords an improved cooling performance based on effusion cooling [154]. In this case a thin film of cool air originates above the aerofoil above the hole edges, resulting in an increase of thermal shielding [25]. This significantly increases turbine entrance temperatures giving higher overall efficiency and reduced fuel consumption. In the past, such cooling holes were exclusively fabricated by EDM however, laser drilling is increasingly being used due to its higher productivity (shortest machining times), superior production line capability and greater flexibility. While EDM has comparatively lower machine tool costs, parallelised machining capability [187] and better process control in terms of break through detection as well as reduced heat affected zones, it is limited to the machining of electrically conductive materials and therefore cannot be applied for ceramic-coated turbine blades.

A method to drill cylindrical cooling holes with conical shaped exits in ceramic-coated turbine blades is the combined use of laser percussion drilling and trepanning operations by applying different laser sources. In this case first a cylindrical through-hole is produced by percussion drilling with a lamp-pumped Nd:YAG-laser, before the shaped hole exit is formed by trepanning. This procedure as suggested by Beck [25] is schematically shown in Fig. 55 together with an

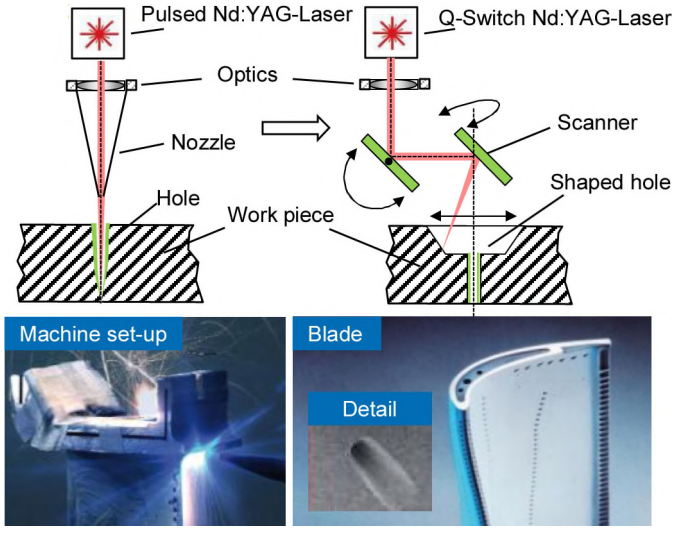


Fig. 55. Principle for process combination of cylindrical drilling and shape hole drilling in one machine set-up and example of high pressure turbine blade with shaped holes. Based on [25,159].

example of application. A Q-switched Nd:YAG laser system with laser pulses of the order of 100 ns pulse duration and high peak powers between 10 and 100 MW/cm^2 are applied for the trepanning setup. In contrast to flash-lamp pumped Nd:YAG solid state lasers with pulse durations of 10–100 μs, the dominating effect causing material removal is ablation and vaporisation of the irradiated material volume. With regard to cooling holes in turbine blades, the combined use affords the possibility to switch dynamically between ablation and melt expulsion during hole formation. This procedure allows the generation of cooling holes with maximum flexibility in terms of the shape, design and drilling depth for improved cooling performance. Additional research has focussed on achieving controlled melt flow by utilisation of a secondary gas jet in order to avoid delamination effects during machining of coated blades [172]. Other process combinations such as sequential laser and mechanical drilling [145], combination of laser and EDM [193] and even EDM with mechanical drilling [67] are also currently under development.

4. Economical process chain analysis and cost modelling

For efficient turbomachinery component manufacture, an economic analysis of individual process technology alternatives as well as the resulting process chains is required. Machining processes with low material removal rates but relatively low machine running costs such as EDM must be evaluated in such a way in order to be competitive against other conventional or advanced manufacturing technologies. Therefore, by performing parallel technological and economic analysis of each operation, optimal processes and process chains can be identified to minimise production costs.

As an example, Fig. 56 shows possible competing machining technologies for the manufacture of a blisk with "hyper-polished" blading. The technologies shown have provisionally been identified as possible variants/alternatives from a technological point of view. While additive manufacturing with complete build-up of blades and water-jet machining from solid are able to produce a rough blade contour, subsequent multi-axis milling could be used for finish machining or for the initial roughing, with conventional or ECM-based polishing applied to produce the finished blades. Alternatively, ECM and PECM (with high MRR) could be employed for the whole process, as they are capable of roughing, finishing and polishing with the same base technology. While all other process technologies need separate machine tools, ECM and PECM can be realised in one set-up. Conversely, such machine tools together with the process and tool electrode design are complex, and therefore more expensive. In order to identify an economic alternative, an appropriate cost model considering all relevant boundary conditions has to be executed and constantly updated when key parameters are changing.

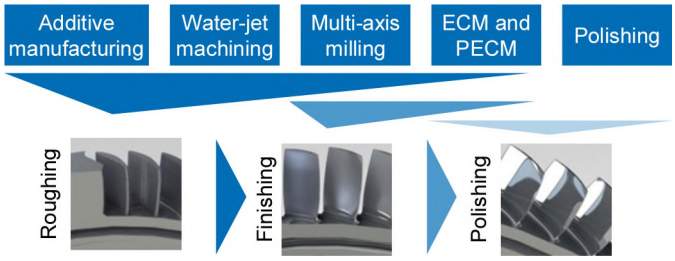
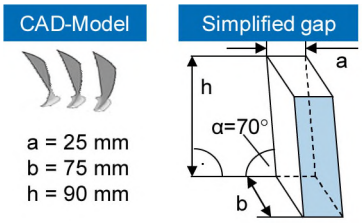


Fig. 56. Example of competing machining technologies for blisk manufacturing process chain of roughing, finishing and polishing.

Such an economical comparison has been carried out for different roughing strategies for blisk gap slotting from solid via multi-axis milling, sinking-EDM and ECM for titanium- and nickel-based blisks. The analysis used a characteristic geometry and the technological key parameters detailed in Fig. 57, the resulting manufacturing costs being calculated as a function of batch size.

Material removal rates have the greatest influence on overall manufacturing costs, as they affect the direct process time and are thus responsible for machine hourly rates and wage costs. In



Material Removal Rate MRR		
mm³/min	Ti-64	Inconel 718
Milling	6035	3401
SEDM	220	500
ECM	4838	4163

Fig. 57. Simplified blisk gap geometry and averaged material removal rates derived from technological analysis, [111].

contrast, tooling costs have limited influence although they have to be taken into account. To allow a comparison, other manufacturing parameters appropriate to blisk manufacture have to be kept constant. These parameters and further assumptions are listed below and provide the basis for the final economic calculation. The idealised blisk possesses 36 blades. Investment/capital costs of machine tools were obtained as official quotations from manufacturers (specialised 5-axis milling machine for turbine industry 1000 k€, SEDM machine 190 k€, ECM machine 400 k€ (plus tooling costs), graphite milling machine 220 k€). Set-up time is equal for each manufacturing technology and amounts to 1 h. Wage costs amount to 35 €/h. For each blisk made of Ti–6Al–4V one milling tool wears out while for Inconel 718 two cutters are required (each at 300 €). Manufacturing and material costs have been considered for SEDM electrodes. The ECM tool operates in the axial direction (marked area). One employee can operate one milling- or ECM machine or alternatively three EDM machines at once. Milling- and ECM machines are used in a two shift production (3200 h/a) and EDM machines in a three shift arrangement (4800 h/a, unmanned EDM production is state of the art) [113].

In Fig. 58, solutions for Ti–6Al–4V and Inconel 718 are shown. Steps in the responses represent critical batch sizes for which full capacity utilisation is reached. Here, the roughing costs per blisk are at a minimum for the respective technology. One-off tool development costs in ECM can be difficult to predict. For this reason, two envelope curves are drawn which consider a lower limit of 100 k€ for tool development costs and an upper limit of 500 k€. Except in the case of small batch sizes from 0 to 20 blisks per year, rough machining via SEDM of Ti–6Al–4V would be simply uneconomic. Milling from solid and ECM – low tool developing costs assumed – are the two technologies in competition. This means that for Ti-based blisks, depending on specific geometries, a closer economic analysis has to be made. For Inconel 718 the choice of the most economical roughing process is more difficult. With low machine tool investment costs and relatively high average material removal rates, SEDM especially for batch sizes up to 400 blisks per year, is a viable alternative. In the case of larger

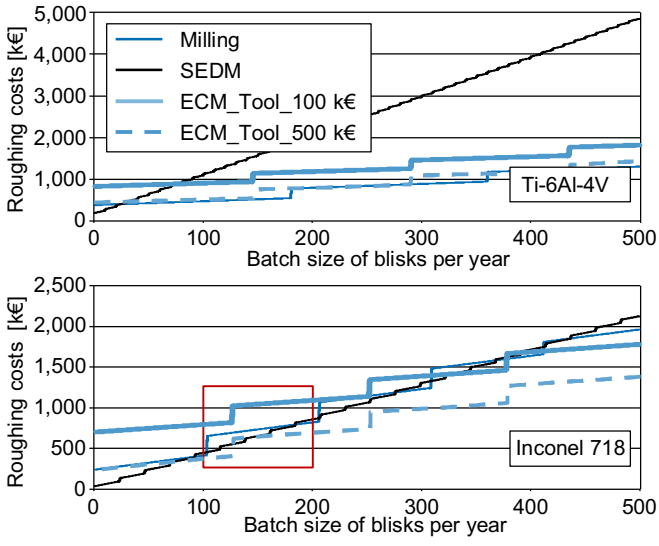


Fig. 58. Roughing costs as a function of batch size for Ti–6Al–4V and Inconel 718 [113].

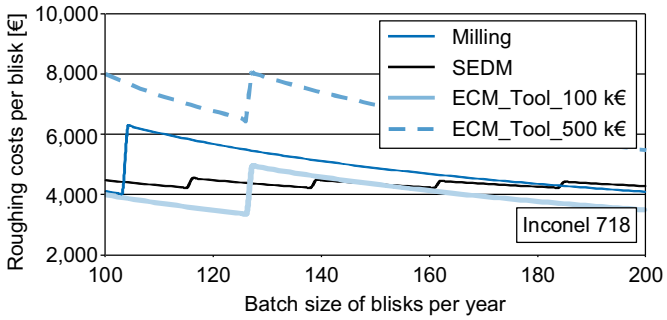


Fig. 59. Roughing costs per blisk as a function of batch size for Inconel 718 (detail according to red box of Fig. 57), [113].

batch sizes, ECM is the most cost-effective technology. Batch sizes of 100–300 require a more detailed analysis [113].

Roughing costs per blisk (Inconel 718) are shown in Fig. 59. Here, costs strongly depend on the batch size as well as investment levels where additional machine tools are required. Technologies like SEDM with low investment costs allow less volatile curve progressions but machine tools and therefore space, is needed more frequently. In the example for a batch size of 200, milling, SEDM and ECM with low tooling outlays reach the same cost level. The local minima of roughing costs – caused by full capacity utilisation – were approximately equivalent. With higher numbers of machine tools, the maximum roughing costs per blisk decrease. This effect is due to the increase in capacity utilisation for each machine tool so that single investment costs are normalised [113].

A similar economic analysis will also have to be carried out for the evaluation of WEDM as a possible alternative technology for fir tree production (assuming proof and acceptance of resulting workpiece functionality) [206]. Although EDM machining time is 10 times longer compared to the established broaching process, the overall costs are estimated to be of the same order of magnitude when taking machine investment costs, tooling and further operating costs into account. Furthermore, WEDM offers higher machining flexibility as well as significantly reduced lead times for new tools and/or new designs.

In addition to the aforementioned characteristics of single operations, further aspects of the complete process chain must be taken into account during technology evaluation. During application of ECM for example, no additional de-burring operation is required in the process chain, as workpiece edges will automatically be rounded. On the other hand, additional washing operations may be necessary. Energy and recycling costs are similarly gaining importance and therefore have to be considered. Recycling of contaminated chips from conventional cutting operations will also need to be critically evaluated [188], as do scrap blocks cut out via WEDM operations. The residual tensile stresses from EDM material removal could be neutralised by subsequent surface finishing operations such as etching, vibro/shot peening, vibratory grinding or abrasive flow machining. Thus, in order to substitute established conventional manufacturing technologies and process chains a comprehensive evaluation of Low Cycle Fatigue (LCF), High Cycle Fatigue (HCF) and Thermal Mechanical Fatigue (TMF) – depending on the chosen turbomachinery component – has to take place relative to the established processes and in dependence on the specific surface integrities. Finally, by using a non-mechanical material removal process, induced forces become less significant, allowing the machining and therefore the design of more filigree and complex geometries, which to date have not been possible by utilising conventional means.

For a comprehensive and balanced economic evaluation of additive manufacturing technologies, novel/new cost model approaches with an extended frame of examination are currently under development. These include the assessment of primary process costs employed to manufacture semi-finished parts for the subtractive process chains as well as consumables, energy and also recycling costs which have up to now, generally not been taken into consideration.

5. Summary and conclusions

The technical capabilities and areas of application of electrochemical, electro-physical and photonic processes have been analysed showing the broad potential of ECM, EDM, additive manufacturing and laser material removal for the manufacture of turbomachinery components. Clear advantages have been identified for their use when machining advanced and difficult-to-cut materials, including high removal and deposition rates, superior geometrical precision and acceptable surface integrity. The case for their selection as alternatives to conventional cutting technologies is further strengthened when considering economic aspects, as outlined in the example for roughing of blisk gaps.

Acknowledgements

The authors would like to express their sincere thanks to R. Perez (GF AgieCharmilles), M. Cuttell (Rolls-Royce), P. Harpham, J. Durrant (Siemens Industrial Turbomachinery); M. Zeis, D. Welling (WZL RWTH Aachen University); H. Krauss, J. Weirather (IWB, TUM) and O. Hentschel, M. Karg, C. Scheitler (LPT, Universität Erlangen) for their assistance in the paper preparation. We would also like to thank the STC-E members involved for their help.

References

[1] Aas KL (2004) Performance of Two Graphite Electrode Qualities in EDM of Seal Slots in a Jet Engine Turbine Vane. *Journal of Materials Processing Technology* 149:152–156.
[2] ACARE (2014) *Aviation in Europe: A vision for 2050.* www.acare4europe.org.
[3] Additive Manufacturing at GE (2011) *Loughborough*. July 12.
[4] Ali S, Hinduja S, Atkinson J, Pandya M (2009) Shaped Tube Electrochemical Drilling of Good Quality Holes. *CIRP Annals – Manufacturing Technology* 58:185–188.
[5] Alkahari MR, Furumoto T, Ueda T, Hosokawa A, Tanaka R, Aziz A, Sanusi M (2012) Thermal Conductivity of Metal Powder and Consolidated Material Fabricated Via Selective Laser Melting. *KEM* 523–524:244–249.
[6] Allen J (2011) The Potential for Aero Engine Component Manufacture Using Additive Layer Manufacturing. *Aerodays Conference*, Madrid.
[7] Amato K, Gaytan S, Murr L, Martinez E, Shindo P, Hernandez J, Collins S, Medina F (2012) Microstructures and Mechanical Behavior of Inconel 718 Fabricated by Selective Laser Melting. *Acta Materialia* 60(5):2229–2239.
[8] Antar MT, Soo SL, Aspinwall DK, Cuttell M, Perez R (2009) Machined Workpiece Surface Integrity Effects Using Advanced Wire EDM. *Proceedings of the 26th International Manufacturing Conference (IMC26)*, Trinity College Dublin, Ireland, 103–110.
[9] Antar MT, Soo SL, Aspinwall DK, Cuttell M, Perez R, Winn AJ (2010) WEDM of Aerospace Alloys Using 'Clean Cut' Generator Technology. *Proceedings of the 16th International Symposium on Electromachining (ISEM XVI)*, 19–23 April, Shanghai, China, 285–290.
[10] Antar MT, Soo SL, Aspinwall DK, Jones D, Perez R (2011) Productivity and Workpiece Surface Integrity when WEDM Aerospace Alloys Using Coated Wires. *Procedia Engineering* 19:3–8.
[11] Antar MT, Soo SL, Aspinwall DK, Sage C, Cuttell M, Perez R, Winn AJ (2012) Fatigue Response of Udimet 720 Following Minimum Damage Wire Electrical Discharge Machining. *Materials and Design* 42:295–300.
[12] ASME Turbo Expo 2013 (2013) *Turbine Technical Conference and Exposition*. Monday, June.
[13] Aspinwall DK, Dewes RC, Mantle AL (2005) The Machining of γ-TiAl Intermetallic Alloys. *CIRP Annals – Manufacturing Technology* 54(1):99–104.
[14] Aspinwall DK, Soo SL, Berrisford AE, Walder G (2008) Workpiece Surface Roughness and Integrity After WEDM of Ti–6Al–4V and Inconel 718 Using Minimum Damage Generator Technology. *Annals of CIRP* 57(1):187–190.
[15] Aspinwall DK, Soo SL, Curtis DT, Mantle AL (2007) Profiled Superabrasive Grinding Wheels for the Machining of a Nickel Based Superalloy. *Annals of CIRP* 56(1):335–338.
[16] Ayesta I, Izquierdo B, Sanchez JA, Ramos JM, Plaza S, Pombo I, Ortega N, Bravo H, Fradejas R, Zamakona I (2013) Influence of EDM Parameters on Slot Machining in C1023 Aeronautical Alloy. *Procedia CIRP* 6:129–134.
[17] Bache MR, Tuppen SJ, Voice WE, Lee HG, Aspinwall DK (2009) Novel Low Cost Procedure for Fabrication of Diffusion Bonds in Ti6/4. *Materials Science and Technology* 25(1):39–49.
[18] Balazic M, Milfelner M, Kopac J (2010) Repair and Manufacture of High Performance Products for Medicine and Aviation with Laser Technology. *AIJSTPME* 3(4):15–22.
[19] Baumgärtner M (2006) *Entwicklung Innovativer ECM-Verfahren für die Herstellung von Leitschaufelsegmenten, Luftfahrtsfoschungsprogr. LuFoIII.*
[20] Baumgärtner M (2010) *Herstellung von Turbinenkomponenten, series of lectures "Ausgewählte Kapitel der Turbomaschinen"*, AKTM, RWTH Aachen University.
[21] Baumgärtner M (2013) *Entwicklung des elektrochemischen Senkens (ECM) und der mechanischen Bearbeitung von Titanaluminiden, Abschlussbericht BMBF-Forschungsvorhaben.*

[22] Bayer E (2014) *Fertigungsprozesse als Schlüsseltechnologie zur Realisierung des Geared Turbo Fan*. Retreived from www.mtu.de.
[23] Bechmann F, Berumen S, Craeghs T, Clijsters S (2012) *Prozessüberwachung und Qualitätssicherung generativ gefertigter Bauteile*, Rapid. Tech, Erfurt.
[24] Bechtold P, Mayer G, Lühring P, Schmidt M (2012) Novel System Technology for Trepanning a Laser Beam at Arbitrary Developments of Angle of Incidence and Lateral Focus Position. *Key Engineering Materials* 523–524:238–243.
[25] Beck T (2011) Laser Drilling in Gas Turbine Blades – Shaping of Holes in Ceramic and Metallic Coatings. *Laser Technik Journal* 3:40–43. (WILEY-VCH, Weinheim).
[26] Bi G, Gasser A (2011) Restoration of Nickel-Base Turbine Blade Knife-edges with Controlled Laser Aided Additive Manufacturing. *Physics Procedia* 12:402–409.
[27] Bi G, Schürmann B, Gasser A, Wissenbach K, Poprawe R (2007) Development and Qualification of a Novel Laser-Cladding Head with Integrated Sensors. *International Journal of Machine Tools & Manufacture* 47:555–561.
[28] Bilgi DJ, Jain VK, Shekhar R, Mehrotra S (2004) Electrochemical Deep Hole Drilling in Super Alloy for Turbine Application. *Journal of Materials Processing Technology* 149:445–452.
[29] *Boeing Current Market Outlook 2013-2032*, (2013), . www.boeing.com/cmo.
[30] Bogoveev NA, Firsov AG, Filatov EI, Tikhonov AS (2001) Computer Support for "All-Round" ECM Processing of Blades. *Journal of Materials Processing Technology* 109:324–326.
[31] Bradley A (2010) *Engine Design for the Environment*, RAeS, Hamburg. June.
[32] Broichhausen K (2004) *Innovationsforum 'Flugtriebwerkstechnik in Brandenburg' Perspektiven für die Einbindung von KMU's in die Triebwerksindustrie, Conference: Brandenburgische TU Cottbus 7–8. Dezember*.
[33] Burger M (2010) *Präzise Elektrochemische Bearbeitung (PECM) komplexer Strukturbauteile*, (Dissertation) TU München, München.
[34] Burger M, Koll L, Werner EA, Platz A (2012) Electrochemical Machining Characteristics and Resulting Surface Quality of the Nickel-Base Single-Crystalline Material LEK94. *Journal of Manufacturing Processes* 14:62–70.
[35] Burger M, Platz A, Werner E (2007) *Herstellung/Nachbearbeitung von Turbinenblisks durch Präzises Elektrochemisches Bearbeiten*, TUM. Retrieved from http://www.wkm.mw.tum.de/forschung/postergalerie/.
[36] Bußmann M, Bayer E (2013) *Market-Oriented Blisk Manufacturing – A Challenge for Production Engineering*, MTU Aero Engines.
[37] Bußmann M, Kraus J, Bayer E (2005) *An Integrated Cost-Effective Approach to Blisk Manufacturing*. Retreived from www.mtu.de.
[38] Bußmann M, Bayer E (2009) *Blisk Production of the Future Technological and Logistical Aspects of Future-Oriented Construction and Manufacturing Processes of Integrally Bladed Rotors*. Retrieved from www.mtu.de.
[39] Chakradhar D, Venu Gopal A (2010) Design and Optimization of Process Parameters in Electrochemical Machining of Inconel 625 Alloy Using Taguchi Method. *Proceedings of the 16th ISEM*, Shanghai, China, 373–377.
[40] Chivel Y, Smurov I (2010) On-Line Temperature Monitoring in Selective Laser Sintering/Melting. *Physics Procedia* 5(5, Part B):515–521.
[41] Clark D, Whittaker MT, Bache MR (2012) Microstructural Characterization of a Prototype Titanium Alloy Structure Processed via Direct Laser Deposition (DLD). *Metallurgical and Materials Transactions: B* 43:388–396.
[42] Clifton D, Mount AR, Jardine DJ, Roth R (2000) Electrochemical Machining of Gamma Titanium Aluminide Intermetallics. *Journal of Materials Processing Technology* 108:338–348.
[43] *Components for Compressors and Turbines*, (2013), . Retrieved from www.leistritz.com.
[44] Cooke A (2010) Variability in the Geometric Accuracy of Additively Manufactured Test Parts. *Proceedings of The 21st Annual Solid Freeform Fabrication Symposium*, An Additive Manufacturing Conference, Austin TX, 1–12.
[45] Craeghs T, Bechmann F, Berumen S, Kruth JP (2010) Feedback Control of Layerwise Laser Melting Using Optical Sensors. *Physics Procedia* 5:505–514.
[46] Craeghs T, Clijsters S, Yasa E, Kruth JP (2011) Online Quality Control of Selective Laser Melting. *Solid Freeform Fabrication: Proceedings*, University of Texas, Austin.
[47] Crosby HC (1985) Wire-Cut and Vertical CNC EDM Systems: Merging Technologies. *Proceedings of the Conference on Non Traditional Machining*, December 2–3, Cincinnati, USA, 43–51.
[48] Curtis DT, Soo SL, Aspinwall DK, Huber C, Fuhlendorf J, Grimm A (2008) Production of Complex Blade Mounting Slots in Turbine Disks Using Novel Machining Techniques. *Proceedings of the 3rd International CIRP High Performance Cutting Conference, Vol. 1*, Dublin, Ireland, 219–228.
[49] Curtis DT, Soo SL, Aspinwall DK, Sage C (2009) Electrochemical Superabrasive Machining of a Nickel-Based Aeroengine Alloyusing Mounted Grinding Points. *CIRP Annals – Manufacturing Technology* 58(1):173–176.
[51] D'Amario R (2008) Method and Apparatus for Generating Machining Pulses for Electrical Discharge Machining, European Patent EP 1719570.
[52] Dausinger F, Lichtner F, Lubatschowski H (2004) Femtosecond Technology for Technical and Medical Applications. *Topics in Apllied Physics*, 96 Springer. ISBN: 978-3-540-20114-4.
[54] Dilba D (2011) Schnelle Schichtarbeit. *MTU Report* 2011(1):20–25. http://www.mtu.de/de/take-off/report/archive/2011_1.pdf.
[55] Dilba D (2012) *Höchste Präzision. Report MTU Aero Engines*. Retrieved from www.mtu.de.
[56] Ding S, Yuan R, Li Z, Wang K (2006) CNC Electrical Discharge Rough Machining of Turbine Blades. *Proceedings of the IMechE Part B: Journal of Engineering Manufacture* 220(7):1027–1034.
[57] Dinwiddie RB, Dehoff RR, Lloyd PD, Lowe LE, Ulrich JB, Stockton GR, Colbert FB (2013) *Thermographic In-Situ Process Monitoring of the Electron-Beam Melting Technology Used in Additive Manufacturing*, SPIE DSS: 87050K.
[58] Domack MS, Baughman JM (2005) Development of Nickel-Titanium Graded Composition Components. *Rapid Prototyping Journal* 11(1):41–51.
[59] ECM/PECM Technologie Polieren (2011) Entgraten, 3D-Konturen, EMAG ECM.
[60] Electrochemical Machining (2013) Retrieved from http://www.koeppern-international.com
[61] Electrochemical Machining (ECM) (2014) *Leistritz Turbomaschinen Technik*. Retrieved from www.leistritz.com.
[62] Elektrochemisches Abtragen (2009) *Verein Deutscher Ingenieure VDI-Richtlinie 3401-1*(Entwurf) .
[63] EMAG's ECM/PECM Machines (2013) Retrieved from http://www.online-amd.com/Article.aspx?article_id=132602.
[64] FAA Continuous Lower Energy, Emissions & Noise (CLEEN) Technologies (2012) *Rolls-Royce Programm Overview*. November 8, www.Rolls-royce.com.
[65] Fleischer J (2011) Erodierbohren – Neue Wege und Anwendungsbeispiele. *Fachtagung Funkenerosion*WZL RWTH Aachen University, Aachen.
[66] Fonda P, Wang Z, Yamazaki K, Akutsu Y (2008) A Fundamental Study on Ti–6Al–4V's Thermal and Electrical Properties and Their Relation to EDM Productivity. *Journal of Materials Processing Technology* 202:583–589.
[67] Garzon M (2011) *Integ-Micro Project: New High-Precision Micro-Machining Technologies*, EMO Hannover, Germany.
[68] Gasser A, Backes G, Kelbassa I, Weisheit A, Wissenbach K (2010) Laser Additive Manufacturing: Laser Metal Deposition (LMD) and Selective Laser Melting (SLM) in Turbo-Engine Applications. *Laser Technik Journal* 7(2):58–63. (WILEY-VCH).
[69] Gasser A, Kelbassa I, Wissenbach K, Witzel J, Göbel M (2012) *Additive Manufacturing in Turbo-Engine Applications*, AKL/EU Innovation Forum, Aachen.
[70] GE Aviation (2013) *GE Aviation Signs Additive Manufacturing Cooperative Agreement with Sigma Labs. Press Release*, GE Aviation, Evendale, Ohio.
[71] GE Aviation (2013) *GE Aviation Signs Additive Manufacturing Cooperative Agreement with Sigma Labs*.
[72] Giese C (2005) *Verfahrensvergleich EDM/ECM im industriellen Umfeld – Anwendungsgebiete von ECM, Fachtagung Funkenerosion*, RWTH Aachen.
[73] GKN Aerospace Capabilities (2010) Retrieved from www.gknaerospace.com.
[74] Gmelin T (2013) *PECM – Anwendungsmöglichkeiten und Grenzen im Ver-gleich zur Funkenerosion. 9. Fachtagung Funkenerosion*, WZL, RWTH, Aachen.
[75] Gong X, Anderson T, Chou K (2012) Review on Powder-Based Electron Beam Additive Manufacturing Technology. *ASME/ISCIE International Symposium on Flexible Automation*, 507–515.
[76] Guo ZN, Lee TC, Yue TM, Lau WS (1997) A Study of Ultrasonic-Aided Wire Electrical Discharge Machining. *Journal of Materials Processing Technology* 63:823–828.
[77] Han F, Wachi S, Kunieda M (2004) Improvement of Machining Characteristics of Micro-EDM Using Transistor Type Isopulse Generator and Servo Feed Control. *Precision Engineering* 28:378–385.
[78] Han GC, Soo SL, Aspinwall DK, Bhaduri D (2013) Research on the Ultrasonic Assisted WEDM of Ti–6Al–4V. *Advanced Materials Research* 797:315–319.
[79] Hascalık A, Caydas U (2007) A Comparative Study of Surface Integrity of Ti–6Al–4V Alloy Machined by EDM and AECG. *Journal of Materials Processing Technology* 190:173–180.
[80] Hascalik A, Caydas U (2007) Electrical Discharge Machining of Titanium Alloy (Ti–6Al–4V). *Applied Surface Science* 253:9007–9016.
[81] Henne J (2013) Gearing Up for High Volume GTF™ Production. *21st ISABE Conference*, Busan, Korea.
[82] Hess T (2012) Aero Engine Parts Made of SLM – Status Quo and Future Potential. *International Laser Technology Congress AKL'12 Aachen*.
[83] Heuer J, Fili W (2006) Konstruieren ohne fertigungstechnisches Limit. *Konstruktion Zeitschrift für Produktentwicklung und Ingenieur-Werkstoffe*, 4.
[84] Hewidy MS, El-Taweel TA, El-Safty MF (2005) Modelling the Machining Parameters of Wire Electrical Discharge Machining of Inconel 601 Using RSM. *Journal of Materials Processing Technology* 169:328–336.
[85] *High-Tech Development and Manufacturing for Aero and Industrial Gas Turbine Components*, (2010), Sulzer ELDIM.
[86] High-tech made by MTU (2011) e-Paper. Retrieved from: www.mtu.de
[87] Hinduja S, Kunieda M (2013) Modelling of ECM and EDM Processes. *CIRP Annals – Manufacturing Technology* 62(2):775–797.
[88] Ho KH, Newman ST (2003) State of the Art Electrical Discharge Machining (EDM). *International Journal of Machine Tools and Manufacture* 43(13):1287–1300.
[89] Horn A, Weichenhain R, Albrecht S, Kreutz EW, Michel J, Niessen M, Kostrykin V, Schulz W, Etzkorn A, Bobzin K, Lugscheider E, Poprawe R (2000) Microholes in Zirconia Coated Ni-Superalloys for Transpiration Cooling of Turbine Blades. *Proceedings of the SPIE 4065, High-Power Laser Ablation III*, 218.
[90] Hrabe N, Quinn T (2013) Effects of Processing on Microstructure and Mechanical Properties of a Titanium Alloy (Ti6Al4V) Fabricated Using EBM, Part 1: DISTANCE from Build Plate and Part Size. *Materials Science and Engineering: A* 573:264–270.
[91] Hrabe N, Quinn T (2013) Effects of Processing on Microstructure and Mechanical Properties of a Titanium Alloy (Ti–6Al–4V) Fabricated Using Electron Beam Melting (EBM). Part 2: Energy Input, Orientation, and Location. *Materials Science and Engineering: A* 573:271–277.
[92] Hubscher B (2012) *NASA's Space Launch System Using Futuristic Technology to Build the Next Generation of Rockets*.
[93] Innovative Technologies for Future Alloys (2013). Retrieved from http://www.turbinentechnik.com/files/alloy_folder.pdf.
[94] Izquierdo B, Plaza S, Sanchez JA, Pombo I, Ortega N (2012) Numerical Prediction of Heat Affected Layer in the EDM of Aeronautical Alloys. *Applied Surface Science* 259:780–790.
[95] Jabbaripoura B, Sadeghia MH, Shabgardb MR, Faraji H (2013) Investigating Surface Roughness Material Removal Rate and Corrosion Resistance in PMEDM of-TiAl Intermetallic. *Journal of Manufacturing Processes* 15: 56–68.
[96] Jain VK, Chavan A, Kulkarni A (2007) Experimental and Analytical Study of Contoured Holes by Shaped Tube Electrochemical Drilling Process. *Proceedings of the 15th Int Symp on Electromachining*, Pittsburgh, USA, 315–318.

[97] Jawahir IS, Brinksmeier E, M'Saoubi R, Aspinwall DK, Outerio JC, Meyer D, Umbrello D, Jayal AD (2011) Surface Integrity in Material Removal Processes: Recent Advances. *CIRP Annals – Manufacturing Technology* 60(2):603–626.

[98] Jefferies R (2013) Continuous Lower Energy, Emissions and Noise (CLEEN) Program. *USACA Spring Association Meeting, 21 May*.

[99] Jones J, McNutt P, Tosi R, Perry C, Wimpenny D (2012) *Remanufacture of Turbine Blades by Laser Cladding, Machining and In-Process Scanning in a Single Machine*. Retrieved from www.dora.dmu.ac.uk.

[100] Joyce D (2012) GE Aviation. *Barclays Capital Industrial Select Conference*.

[102] Kao JY, Tsao CC, Wang SS, Hsu CY (2010) Optimisation of the EDM Parameters on Machining Ti–6Al–4V with Multiple Quality Characteristics. *International Journal of Advanced Manufacturing Technology* 47:395–402.

[103] Kelbassa I, Albus P, Dietrich J, Wilkes J (2008) Manufacture and Repair of Aero Engine Components Using Laser Technology. *Proceedings of the 3rd Pacific Conference on Application of Lasers and Optics*, 208–212.

[104] Klocke F, König W (2007) *Fertigungsverfahren 3: Abtragen, Generieren und Lasermaterialbearbeitung*, Springer, Berlin. ISBN 3-540-23492-6.

[105] Klocke F, Welling D, Dieckmann J (2011) Comparison of Grinding and Wire-EDM Concerning Fatigue Strength and Surface Integrity of Machined Ti6Al4V Components. *Procedia Engineering* 19:184–189.

[106] Klocke F, Welling D, Dieckmann J, Veselovac D, Perez R (2012) Developments in Wire-EDM for the Manufacturing of Fir Tree Slots in Turbine Discs Made of Inconel 718. *Key Engineering Materials* 504–506:1177–1182.

[107] Klocke F, Welling D, Klink A, Veselovac D, Nöthe T, Perez R (2014) Evaluation of Advanced Wire-EDM Capabilities for the Manufacture of Fir Tree Slots in Inconel 718. *Submitted to 6th CIRP International Conference on High Performance Cutting*, Berkely, USA.

[108] Klocke F, Zeis M, Harst S, Herrig T, Klink A (2013) Analysis of the Simulation Accuracy of Electrochemical Machining Processes Based on the Integration Level of Different Physical Effects. *M. Scripts Precision and Microproduction Engineering 7, Fraunhofer IWU*, 165–170. ISBN 978-3-942267-95-3.

[109] Klocke F, Zeis M, Harst S, Klink A, Veselovac D, Baumgärtner M (2013) Modeling and Simulation of the Electrochemical Machining (ECM) Material Removal Process for the Manufacture of Aero Engine Components. *Procedia* 8:265–270.

[110] Klocke F, Zeis M, Klink A (2012) Technological and Economical Capabilities of Manufacturing Titanium- and Nickel-Based Alloys Via Electrochemical Machining (ECM). *Key Engineering Materials* 504–506:1237–1242.

[111] Klocke F, Zeis M, Klink A, Veselovac D (2012) Technological and Economical Comparison of Roughing Strategies via Milling, EDM and ECM for Titanium- and Nickel-Based Blisks. *Procedia CIRP* 2:98–101.

[112] Klocke F, Zeis M, Klink A, Veselovac D (2013) Experimental Research on the Electrochemical Machining of Modern Titanium- and Nickel-Based Alloys for Aero Engine Components. *Procedia CIRP* 6:369–373.

[113] Klocke F, Zeis M, Klink A, Veselovac D (2013) Technological and Economical Comparison of Roughing Strategies Via Milling, Sinking-EDM, Wire-EDM and ECM for Titanium- and Nickel-Based Blisks. *CIRP JMST* 6(3):198–203.

[114] Krauss H, Eschey C, Zäh MF (2012) Thermography for Monitoring the Selective Laser Melting Process. *Solid Freeform Fabrication: Proceedings*University of Texas, Austin.

[115] Krauss H, Zäh MF (2013) Multi-target Optimization and Process Window Analysis in Selective Laser Melting of High-performance Parts. *22nd International Conference on Production Research (ICPR 22)*.

[116] Kremer D, Bazine G, Moisan A, Bessaguet L, Astier A, Thanh NK (1983) Ultrasonic Machining Improves EDM Technology. *Proceedings of the 7th International Symposium on Electromachining (ISEM VII)*, 2–14 April, Birmingham, UK, 67–76.

[117] Kremer D, Lhiaubet C, Moisan A (1991) A Study of the Effect of Synchronizing Ultrasonic Vibrations with Pulses in EDM. *Annals of CIRP* 40(1):211–214.

[118] Kruth JP, Levy G, Klocke F, Childs THC (2007) Consolidation Phenomena in Laser and Powder-Bed Based Layered Manufacturing. *CIRP Annals* 56(2):730–759.

[119] Kunieda M, Lauwers B, Rajurkar KP, Schumacher BM (2005) Advancing EDM Through Fundamental Insight into the Process. *Annals of CIRP* 54(2):64–87.

[120] Kuriakose S, Shunmugam MS (2004) Characteristics of Wire-Electro Discharge Machined Ti6Al4V Surface. *Materials Letters* 58:2231–2237.

[121] Lakomiec M (2013) *Serienfertigung von Triebwerksteilen mittels Laserstrahlschmelzen*, VDI Fachkonferenz Additive Manufacturing – Vom Prototypen bis zur Großserie mit generativen Fertigungsverfahren, Duisburg.

[122] Lauwers B, Klocke F, Klink A, Tekkaya AE, Neugebauer R, Mcintosh D (2014) Hybrid Processes in Manufacturing. *CIRP Annals – Manufacturing Technology* 63(2):561–583.

[123] Leahy J (2013) *Global Market Forecast 2013–2032*. www.airbus-group.com.

[124] Lee HG, Simao J, Aspinwall DK, Dewes RC, Voice W (2004) Electrical Discharge Surface Alloying. *Journal of Materials Processing Technology* 149:334–340.

[125] Leigh S, Sezer K, Li L, Grafton-Reed C, Cuttell M (2010) Recast and Oxide Formation in Laser-Drilled Acute Holes in CMSX-4 Nickel Single-Crystal Superally. *Proceedings of the IMechE, Part B: Journal of Engineering Manufacture 224* 7:1005–1016.

[126] Levy GN (2010) The Role and Future of the Laser Technology in the Additive Manufacturing Environment. *Physics Procedia* 5:65–80.

[127] Li J, Wang HM (2010) Microstructure and Mechanical Properties of Rapid Directionally Solidified Ni-Base Superalloy Rene 41 by Laser Melting Deposition Manufacturing. *Materials Science and Engineering: A* 527:4823–4829.

[128] Li L, Guo YB, Wei XT, Li W (2013) Surface Integrity Characteristics in Wire-EDM of Inconel 718 at Different Discharge Energy. *Procedia CIRP* 6:221–226.

[129] Lin YC, Yan BH, Chang YS (2000) Machining Characteristics of Titanium Alloy (Ti–6Al–4V) Using a Combination Process of EDM with USM. *Journal of Materials Processing Technology* 104:171–177.

[130] Liu K, Ferraris E, Peirs J, Lauwers B, Reynaerts D (2008) Precision Manufacturing of the Ultra Miniature Gas Turbine in Ceramic Composite for the Micro Power Generation System. *Proceedings of the Euspen International Conference, Zurich*.

[131] Liu X, Kang X, Zhao W, Liang W (2013) Electrode Feeding Path Searching for 5-Axis EDM of Integral Shrouded Blisks. *Procedia CIRP* 6:107–111.

[132] Majundar JD (2012) *Laser Assisted-Fabrication of Materials*, Springer, Berlin.

[133] Mantle AL, Abboud E, Aspinwall DK (1997) Productivity and Workpiece Surface Integrity Effects When Electrical Discharge Wire Machining a Gamma Titanium Aluminide. *Proceedings of the 14th Conference of the Irish Manufacturing Committee (IMC-14)*, 3–5 September, Trinity College Dublin, Ireland, 443–450.

[135] Meiners W (1999) *Direktes Selektives Laser-Sintern Einkomponentiger Metallischer Werkstoffe*, Shaker, Aachen.

[136] Meiners W (2012) *High Power SLM Machining of Inconel 718, Annual Report*, Fraunhofer-Institut für Lasertechnik ILT.

[137] Metcut Research Associates (1980) *Machining Data Handbook*, 3rd ed., vol. 2. MDC, Cincinnati, OH.

[138] Mühlbauer G (2011) *Funkenerosion im Triebwerksbau. Workshop Mikrofunkenerosion 14*, TU, Berlin. April.

[139] Mumtaz K, Hopkinson N (2010) Selective Laser Melting of Thin Wall Parts Using Pulse Shaping. *Journal of Materials Processing Technology* 210(2):279–287.

[140] Mumtaz KA, Hopkinson N (2007) Laser Melting Functionally Graded Composition of Waspaloy and Zirconia Powders. *Journal of Material Science* 42(18):7647–7656.

[141] Murr LE, Gaytan SM, Ceylan A, Martinez E, Martinez JL, Hernandez DH, Machado BI, Ramirez DA, Medina F, Collins S, Wicker RB (2010) Characterization of Titanium Alluminide Alloy Components Fabricated by Additive Manufacturing Using Electron Beam Melting. *Acta Materialia* 58:1887–1894.

[142] Murthy VSR, Philip PK (1983) Pulse Train Analysis in Ultrasonic Assisted EDM. *International Journal of Machine Tools and Manufacture* 27(4):469–477.

[143] NCMT (2013) *Deep-Hole EDM Drilling of Turbine Components is Seven Times Faster*. Retrieved from http://www.ncmt.co.uk.

[144] Okane M, Goto A (2008) Development of MS Coating for Aircraft Engine Parts. *Mitsubishi Electric Advance Mechatronics* 123. ISSN 1345-3041.

[145] Okasha MM, Mativenga PT, Driver N, Li L (2010) Sequential Laser and Mechanical Micro-Drilling of Ni Superalloy for Aerospace Application. *CIRP Annals – Manufacturing Technology* 59:199–202.

[146] Ott M (2012) *Multimaterialverarbeitung bei der additiven strahl- und pulverbettbasierten Fertigung*, Dissertation, TU, München.

[147] Ott M, Zaeh MF (2010) Multi-Material Processing in Additive Manufacturing. in Bourell DL, et al. (Eds.) *2010 – Proceedings of the 21st SFF Symposium*, Austin, University of Texas at Austin 195–203.

[148] Pandey A, Singh S (2010) Current Research Trends in Variants of Electrical Discharge Machining: A Review. *International Journal of Engineering Science and Technology* 2(6):2172–2191.

[149] Pattavanitch J, Hinduja S (2012) Machining of Turbulated Cooling Channel Holes in Turbine Blades. *CIRP Annals – Manufacturing Technology* 61:199–202.

[150] Paul MA, Aspinwall DK (1998) Arc Sawing Performance Evaluation and Machine Design. *Proceedings of the 12th International Symposium on Electromachining (ISEM XII)*, 11–13 May, Aachen, Germany, 407–416.

[151] Paul MA, Liang WS, Aspinwall DK (1998) Arc Sawing Applications and the Development of Arc Profile Machining. *Proceedings of the 4th International Conference on Advances in Materials and Processing Technology (AMPT)*, 24–28 August, Kuala Lumpur, Malaysia, 819–826.

[152] Platz A, Feiling N (2013) *Precise Electrochemical Machining of Nickel Base Integrated Blade Compressor Rotors*, Precision and Microproduction Engineering 7, Fraunhofer IWU, Chemnitz23–32. ISBN 978-3-942267-95-3.

[153] Poprawe R (2005) *Lasertechnik für die Fertigung-Grundlagen, Perspektiven und Beispiele für den innovativen Ingenieur*, Springer, Berlin.

[154] Poprawe R, Kelbassa I, Walther K, Witty M, Bohn D, Krewinkel R (2008) Optimising and Manufacturing a Laser-Drilled Cooling Hole Geometry for Effusion-Cooled Multi-Layer Plates. *Proceedings of the 12th ISROMAC Hawai, 17–22 February*, 1–10.

[155] Prihandana GS, Mahardika M, Hamdi M, Mitsui K (2011) Effect of Low-Frequency Vibration on Workpiece in EDM Processes. *Journal of Mechanical Science and Technology* 25(5):1231–1234.

[156] Qi H, Azer M, Singh P (2010) Adaptive Toolpath Deposition Method for Laser Net Shape Manufacturing and Repair of Turbine Compressor Airfoils. *International Journal of Advanced Manufacturing Technology* 48:121–131.

[157] Ramakrishnan R, Karunamoorthy L (2008) Modeling and Multi-Response Optimization of Inconel 718 on Machining of CNC WEDM Process. *Journal of Materials Processing Technology* 207:343–349.

[158] Reed RC (2006) *The Superalloys*, Cambridge University Press, Cambridge.

[159] Richter KH (2008) Laser Material Processing in the Aero Engine Industry. Established Cutting-Edge and Emerging Applications. *Proceedings of the 3rd Pacific International Conference on Application of Lasers and Optics*.

[160] Richter KH (2010) Using the Laser for Build-Up. Established and Emerging Applications at MTU Aero Engines. *International Laser Technology Congress AKL'10*, Aachen.

[161] Richter KH, Orban S, Nowotny S (2004) Laser Cladding of the Titanium Alloy Ti6242 to Restore Damaged Blades. *Proceedings of the 23rd International Congress on Applications of Lasers and Electro-Optics*.

[162] Rodriguez E, Medina F, Espalin D, Terrazas C, Muse D, Henry C, MacDonald E, Wicker R (2012) Integration of a Thermal Imaging Feedback Control System in Electron Beam Melting. *Solid Freeform Fabrication: Proceedings*University of Texas, Austin.

[163] *Rolls Royce – The Jet Engine*, (2005), . ISBN: 0902121235.

[164] Rolls Royce Market Outlook 2012-31 (2012) www.rolls-royce.com.

[165] Sánchez JA, Plaza S, Gil R, Ramos JM, Izquierdo B, Ortega N, Pombo I (2013) Electrode Set-Up for EDM-Drilling of Large Aspect-Ratio Microholes. *Procedia CIRP* 6:275–280.

[166] Sarkar S, Mitra S, Bhattarcharyya B (2005) Parametric Analysis and Optimization of Wire Electrical Discharge Machining of γ-Titanium Aluminide Alloy. *Journal of Materials Processing Technology* 159:286–294.

[167] Sarkar S, Sekh M, Mitra S, Bhattacharyya B (2008) Modeling and Optimization of Wire Electrical Discharge Machining of gTiAl in Trim Cutting Operation. *Journal of Materials Processing Technology* 205:376–387.

[168] Schubert A, Hackert-Oschätzchen M, Meichsner G, Zinecker M, Edelmann J (2011) Precision and Micro ECM with Localized Anodic Dissolution. in Slabe JM, (Ed.) *TECOS Slovenian Tool and Die Development Centre, Celje: Proceedings of the 8th International Conference on Industrial Tools and Material Processing Technologies*, 193–196. ISBN: 978-961-6692-02-1.

[169] Schwerdtfeger JV, Singer RF, Körner C (2012) In Situ Flaw Detection by IR-Imaging During Electron Beam Melting. *Rapid Prototyping Journal* 18(4):259–263.

[170] Sen B, Kiyawat N, Singh PK, Mitra S, Ye JH, Purkait P (2003) Developments in Electric Power Supply Configurations for Electrical-Discharge-Machining (EDM). *Proceedings of the Fifth International Conference on Power Electronics and Drive Systems (PEDS 2003) – Vol. 1*, 17–20 November, Singapore, 659–664.

[171] Sen M, Shan HS (2005) A Review of Electrochemical Macro- to Micro-Hole Drilling Processes. *International Journal of Machine Tools & Manufacture* 45:137–152.

[172] Sezer HK, Li L, Leigh S (2009) Twin Gas Jet-Assisted Laser Drilling Through Thermal Barrier-Coated Nickel Alloy Substrates. *International Journal of Machine Tools & Manufacture* 49:1126–1135.

[173] Shen N, Chou K (2012) Numerical Thermal Analysis in Electron Beam Additive Manufacturing with Preheating Effects. *Solid Freeform Fabrication: Proceedings*University of Texas, Austin.

[174] Shepeleva L, Medres B, Kaplan WD, Bamberger M, Weisheit A (2000) Laser Cladding of Turbine Blades. *Surface and Coatings Technology* 125:45–48.

[175] Sieber J (2014) *Langfristige Sicherung des Luftverkehrs durch neue Antriebstechnologien und alternative Brennstoffe*. Retrieved from www.mtu.de.

[176] Sivakumar KM, Gandhinathan R (2013) Establishing Optimum Process Parameters for Machining Titanium Alloys (Ti–6Al–4V) in Spark Electrical Discharge Machining. *International Journal of Engineering and Advanced Technology* 2(4):201–204.

[177] Soo SL, Antar MT, Aspinwall DK, Sage C, Cuttell M, Perez R, Winn AJ (2013) The Effect of Wire Electrical Discharge Machining on the Fatigue Life of Ti–6Al–2Sn–4Zr–6Mo Aerospace Alloy. *Procedia CIRP* 6:215–219.

[178] Soo SL, Hood R, Aspinwall DK, Voice WE, Sage C (2011) Machinability and Surface Integrity of RR1000 Nickel Based Superalloy. *CIRP Annals – Manufacturing Technology* 60:89–92.

[179] Steffens K, Platz A, Buckl F, (2004) Feinbearbeitungsverfahren – Schlüsseltechnologien für moderne Luftfahrtverdichter. MTU Aero Engines. www.mtu.de.

[180] Steffens K, Walther R (2003) *Driving the Technological Edge in Airbreathing Propulsion*. Retrieved from www.mtu.de.

[181] Steffens K, Wilhelm H (2013) *Werkstoffe, Oberflächentechnik und Fertigungsverfahren für die nächste Generation von Flugtriebwerken*. Retrieved from www.mtu.de.

[182] Stimper B (2014) *Using Laser Powder Cladding to Build Up Worn Compressor Blade Tips MTU Aero Engines*. Retrieved from www.mtu.de.

[183] Su W (2002) *Layered Fabrication of Tool Steel and Functionally Graded Materials with a Nd: YAG Pulsed Laser*, (PhD thesis) Loughborough University, Loughborough, UK.

[184] Taberno I, Lamikiz A, Martinez S, Ukar E, Figueras J (2011) Evaluation of the Mechanical Properties of Inconel 718 Components Built by Laser Cladding. *International Journal of Machine Tools & Manufacture* 51:465–470.

[185] Thanigaivelan R, Arunachalam RM, Karthikeyan B, Loganathan P (2013) Electrochemical Micromachining of Stainless Steel with Acidified Sodium Nitrate Electrolyte. *Procedia CIRP* 6:352–356.

[186] Thoe TB, Aspinwall DK, Killey N (1999) Combined Ultrasonic and Electrical Discharge Machining of Ceramic Coated Nickel Alloy. *Journal of Materials Processing Technology* 92–93:323–328.

[187] Thümmler T (2008) *Herstellung von komplexen Kühlluftbohrungen in Hochdruckturbinenschaufeln*, MTU Aero Engines.

[188] Titan beim Zerspanen nicht länger verschwenden. *Produktion* 41:18. www.produktion.de.

[189] Toller DF (1983) Multi-Small Hole Drilling by EDM. *Proceedings of the 7th International Symposium on Electromachining (ISEM VII)*, 12–14 April, Birmingham, UK, 147–156.

[190] Toyserkani E, Khajepour A (2005) *Laser Cladding*, CRC Press, Boca Raton.

[191] Uhlmann E, Domingos DC (2013) Development and Optimization of the Die-Sinking EDM-Technology for Machining the Nickel-Based Alloy MAR-M247 for Turbine Components. *Procedia CIRP* 6:181–186.

[192] Uhlmann E, Domingos DC (2013) Investigations on Vibration-Assisted EDM – Machining of Seal Slots in High-Temperature Resistant Materials for Turbine Components. *Procedia CIRP* 6:71–76.

[193] Uhlmann E, Oberschmidt D, Langmack M (2013) Complex Bore Holes fabricated by combined Helical Laser Drilling and Micro Electrical Discharge Machining. *28th ASPE Annual Meeting*.

[194] van Tijum R, Pajak T (2008) *The Multiphysics Approach: The Electrochemical Machining Process*, Presentation During COMSOL Conference Hannover.

[195] Verfahren zur Reduzierung von Chrom(VI) bei der ECM-Bearbeitung, Retrieved from http://www.maschinenmarkt.vogel.de

[196] Veselovac D (2013) *Process and Product Monitoring in the Drilling of Critical Aero Engine Components*, (Dissertation) WZL RWTH Aachen University.

[197] Vrancken B, Thijs L, Kruth J-P, van Humbeeck J (2012) Heat Treatment of Ti6Al4V Produced by Selective Laser Melting: Microstructure and Mechanical Properties. *Journal of Alloys and Compounds* 541:177–185.

[198] Walther R (2012) Recent Challenges in Air Breathing Propulsion. *Proceedings of the 14th International Symposium on Transport Phenomena and Dynamics of Rotating Machinery*.

[199] Wang JY, Yu Y, McGeough JA, De Silva A (2007) Experimental Investigation for the Enhancement of Accuracy of Pulse Electrochemical Machining by Improvement of Pulse Power. *Proceedings of the 15th ISEM*, Pittsburgh, USA, 369–373.

[200] Wang MH, Zhub D (2009) Simulation of Fabrication for Gas Turbine Blade Turbulated Cooling Hole in ECM Based on FEM. *Journal of Materials Processing Technology* 209:1747–1751.

[201] Wang Z, Guan K, Gao M, Li X, Chen X, Zeng X (2012) The Microstructure and Mechanical Properties of Deposited-IN718 by Selective Laser Melting. *Journal of Alloys and Compounds* 513:518–523.

[203] Wardono B, Ismail MFB, Liew PJ (2011) An Analysis of EDM Die Sinking Parameters on Ti–6Al–4V. *Proceedings of the International Conference and Exhibition on Sustainable Energy and Advanced Materials (ICESEAM2011)*, Solo, Indonesia, 3–4 October, 367–373.

[204] Wei B, Kozak J, Rajurkar KP (1994) Pulse Electrochemical Machining (PECM) of Ti–6Al–4V Alloy. *Transactions of NAMRI/SME XXII* 141–147.

[205] Wei B, Trimmer AL, Luo Y, Yuan R, Hayashi S, Lamphere M (2010) Advancement in High Speed Electro-Erosion Processes for Machining Tough Metals. *Proceedings of the 16th ISEM*, 19–23 April, Shanghai, China, 193–196.

[206] Welling D (2013) *Drahtfunkenerosive Bearbeitung von Profilnuten in Nickelbasislegierungen. 9. Fachtagung Funkenerosion*, RWTH Aachen University.

[207] Welling D (2014) Results of Surface Integrity and Fatigue Study of Wire-EDM compared to Broaching and Grinding for demanding Jet Engine Components Made of Inconel 718. *Procedia CIRP* 13:339–344.

[208] Westley JA, Atkinson J, Duffield A (2004) Generic Aspects of Tool Design for Electrochemical Machining. *Journal of Materials Processing Technology* 149:384–392.

[209] Winbro Group Technologies (2014) *Series 800 Laser & EDM Datasheet*.

[210] Witzel J, Schopphoven T, Gasser A, Kelbassa I (2011) Development of a Model for Prediction of Material Properties of Laser Cladded Inconel 718 as Related to Porosity in the Bulk Material. *Proceedings of the 30th ICALEO*, Orlando, USA, 275–282.

[211] Witzel J, Schrage J, Gasser A, Kelbassa I (2011) Additive Manufacturing of a Blade-Integrated Disk by Laser Metal Deposition. *Proceedings of 30th International Congress on Applications of Lasers & Electro-Optics*, Orlando, USA, 250–256.

[212] Wohlers T, Gornet T (2011) History of Additive Manufacturing. in Wohlers T, (Ed.) *Wohlers Report: Additive Manufacturing and 3D Printing State of the Industry Annual Worldwide Progress Report*, Wohlers Associates, Fort Collins, CO.

[213] Wohlers TT (2012) *Wohlers Report 2012: Additive Manufacturing and 3D Printing State of the Industry: Annual Worldwide Progress Report*, Wohlers Associates, Fort Collins, CO.

[214] Wollenberg G, Schulze HP, Trautmann HJ, Kappmeyer G (2007) Controlled Current Rise for Pulsed Electrochemical Machining. *Proceedings of the 15th International Symposium on Electromachining*, Pittsburgh, USA.

[215] Xu ZY, Xu Q, Zhu D, Gong T (2013) A High Efficiency Electrochemical Machining Method of Blisk Channels. *CIRP Annals – Manufacturing Technology* 62:187–190.

[216] Xue L, Li Y, Wang S (2011) Direct Manufacturing of Net-Shape Functional Components/Test-Pieces for Aerospace, Automotive and Other Applications. *Proceedings of the 30th ICALEO*, 23–27 October, Orlando, USA, 479–488.

[217] Yang DY, Cao FG, Liu YJ, Yang LG, Zhang K, Zhu YF (2013) Overview on Five-Axis Precision EDM Techniques. *Procedia CIRP* 6:193–199.

[218] Yasa E, Kruth JP, Deckers J (2011) Manufacturing by Combining Selective Laser Melting and Selective Laser Erosion/Laser Re-melting. *CIRP Annals* 60:263–266.

[219] Ye L (1992) Apparatus for electrical machining. US Patent 5128010/1992.

[220] Yu J, Rombouts M, Motmans F (2012) Material Properties of Ti6Al4V Parts Produced by Laser Metal Deposition. *Physics Procedia* 39:416–424.

[221] Yu J, Xiao P, Liao Y, Cheng M (2009) Surface Integrity in Electrical Discharge Machining of Ti–6Al–4V. *Advanced Materials Research* 76–78:613–617.

[222] Yuan R, Wei B, Luo Y, Zhan Y, Xu W, Lamphere M (2010) Advancement in High Speed Electro-Erosion Processes for Machining Tough Metals. *Proceedings of the 16th International Sympsium on Electromachining (ISEM)*, 19–23 April, Shanghai, China, 207–210.

[223] Zaeh MF, Branner G (2010) Investigations on Residual Stresses and Deformations in Selective Laser Melting. *Production Engineering – Research and Development* 4(1):35–45.

[224] Zäh MF, Lutzmann S (2010) Modelling and Simulation of Electron Beam Melting. *Production Engineering – Research and Development* 4(1):15–23.

[225] Zäh MF, Ott M (2011) Investigations on Heat Regulation of Additive Manufacturing Processes for Metal Structures. *CIRP Annals – Manufacturing Technology* 60(1):259–262.

[226] Zhao JS, Xu JW, Zhu YW (2007) Design Optimization of Cathode's Feeding Path of NC-Electrochemical Machining Based on Computer Simulation of Shaping Process. *Proceedings of the 15th International Symposium on Electromach*, Pittsburgh, USA, 365–368.

[227] Zhao W, Go L, Xu H, Li L, Xiang X (2013) A Novel High Efficiency Electrical Erosion Process – Blasting Erosion Arc Machining. *Procedia CIRP* 6:622–626.

[228] Zheng Z, Wang Y, Dong Y, Wang Z (2010) Fabrication of Key Components in Micro Turbine Engine by Using Micro Electrical Discharge Machining (EDM). *Proceedings of the 16th International Symposium on Electromachining*, Shanghai, 587–591.

[229] Zhu D, Zhu D, Xu Z, Zhou L (2013) Trajectory Control Strategy of Cathodes in Blisk Electrochemical Machining. *Canadian Journal of Anaesthesia* 26(4):1064–1070.

[230] Hofmann DC, Borgonia JP, Dillon RP, Suh EJ, Mulder JL, Gardner PB (2013) Methods for Fabricating Gradient Alloy Articles with Multi-Functional Properties, Patent WO 2013/112217 A2.